U.S. Department of Energy
HelioCon
Heliostat Consortium for
Concentrating Solar-Thermal Power

Extending Deflectometry Metrology Capability for CSP

Randy Brost, Braden Smith, Felicia Brimigion, and Anthony Evans
Sandia National Laboratories

conceptional design • components • integration • mass production • heliostat field

Sandia National Laboratories is a multimission laboratory managed and operated by National Technology & Engineering Solutions of Sandia, LLC, a wholly owned subsidiary of Honeywell International Inc., for the U.S. Department of Energy's National Nuclear Security Administration under contract DE-NA0003525.

Sandia Concentrating Solar Optics Laboratory (CSOL)

Mission:

Promote construction of high-performance heliostat fields, by delivering high performance, easy-to-access solutions.

Key products in the works:

- SOFAST – High-resolution mirror slope measurement. Today's focus
- UFACET – High-speed drone-based field inspection.
- Ground truth – Simple methods or objects with known accuracy.
- OpenCSP – Foundation classes, applications, and data for community development.

Thanks

We thank the DOE Solar Technologies Office and the Sandia LDRD program for their support.

SOFAST original developers: Chuck Andraka, Nolan Finch, Julius Yellowhair, others…

TEAM

- Randy Brost
- Braden Smith

Manager:

- Margaret Gordon

Students:

- Ben Bean
- Felicia Brimigion
- Madeline Hwang
- Tristan Larkin
- Estevan Rodrigues

Staff:

- Lam Banh
- Roger Buck
- Robert Crandell
- Anthony Evans
- Luis Garcia Maldonado
- Kevin Good
- Dimitri Madden
- Dave Novick
- Daniel Ray
- Dan Small
- Benson Tso

Heliostat Optical Metrology Problems

Ideal:

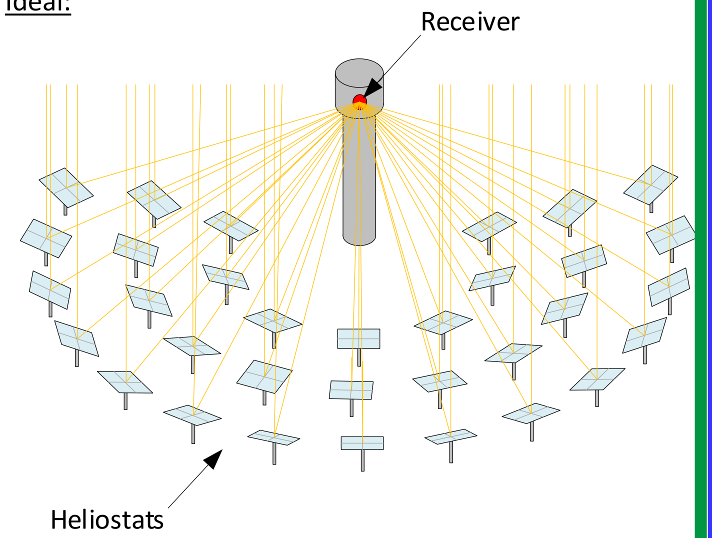

No Error
Heliostats produce tight beams.
All focus on desired target.

⇒ High Temperature (T > 1000 °C)
High Power ($P > 100\ MW_{th}$)

Slope Error:

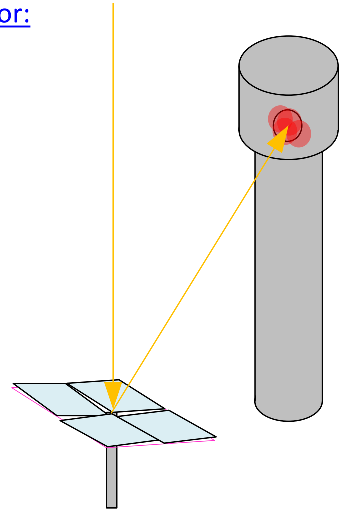

Slope error causes irregular, defocused beam.
Power is not focused in expected location.

Measure:

- Optical slope:

$$f(x, y) \rightarrow \vec{n}_{(x,y)}$$

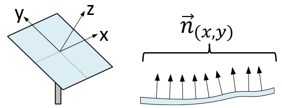

- **Varies with configuration, temperature.**

Corrective actions:

- Design refinement.
- Manufacturing control.
- In-field maintenance (rare).

This Presentation

Pointing Error:

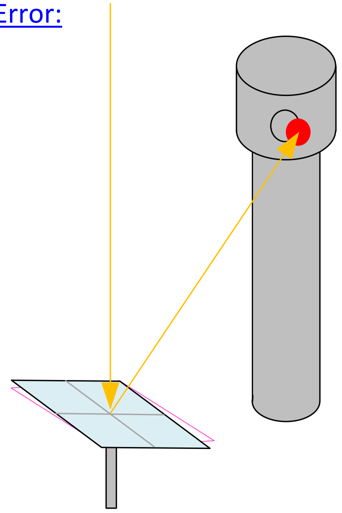

Pointing error causes beam to miss target.
Power is not in expected location.

Measure:

- Correction function:

$$f(c_1, c_2) \rightarrow [\Delta c_1, \Delta c_2]$$

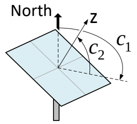

- **For all sun positions in solar year.**
- Two flavors:
  - Offline calibration.
  - Real-time, during operation.

Corrective actions:

- Apply correction function via software control.

Dynamic Effects:

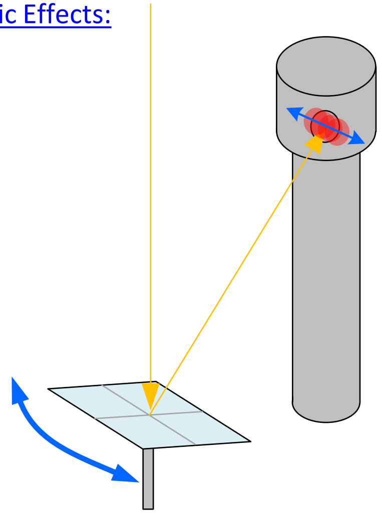

Beam oscillations due to wind or control.
Power location varies over time.

Measure:

- Shape variation with time.
- Pointing variation with time.
- Wind-induced: Flutter response.
- Self-induced: Control dynamics.

Corrective actions:

- Design refinement.
- Operation strategy.

Consequences of optical error:

- Directly reduce temperature and power.
- Spillage can cause damage.
- Unpredictable hot spots, leading to either (a) damage or (b) conservative operation.

Requirements:

- Measurement accuracy must be < 0.01°.
- Measurements must be in situ, daylight, high speed.

Measuring High-Resolution Slope Maps: Background

Example prior papers:

- T. Wendelin, K. May, and R. Gee. Video Scanning Hartmann Optical Testing of State-of-the-Art Parabolic Trough Concentrators. Solar 2006 Conference (ISEC ’06), Denver, Colorado, July 2006. Also NREL NREL/CP-550-39590, June 2006.
- T. März, et al. Validation of Two Optical Measurement Methods for the Qualification of the Shape Accuracy of Mirror Panels for Concentrating Solar Systems. *Journal of Solar Energy Engineering* **133**, August 2011.
- S. Ulmer, et al. Automated High Resolution Measurement of Heliostat Slope Errors. *Solar Energy* **85**, pp. 685-687, 2011.
- C. Andraka, et al. Rapid Reflective Facet Characterization Using Fringe Reflection Techniques. *Journal of Solar Energy Engineering* **136**, February 2014.
- N. S. Finch and C. E. Andraka. Uncertainty Analysis and Characterization of the SOFAST Mirror Facet Characterization System. *Journal of Solar Energy Engineering* **136**, February 2014.
- A.M. Bonanos, M. Faka, D. Abate, S. Hermon, and M.J. Blanco. Heliostat surface shape characterization for accurate flux prediction. *Renewable Energy* **142**, pp. 30-40, 2019.
- M. Montecchi, G. Cara, and A. Benedetti. VISproPT commissioning and SFERA-III WP10 Task3 round-robin on 3D shape measurements: recommended procedure and ENEA results. ENEA Report TERIN-STSN/2022/14, November 2022.
- CSP Services. QDec-M. https://www.cspservices.de/wp-content/uploads/CSPS-QDec.pdf.

DLR/CSP Services Accomplishments

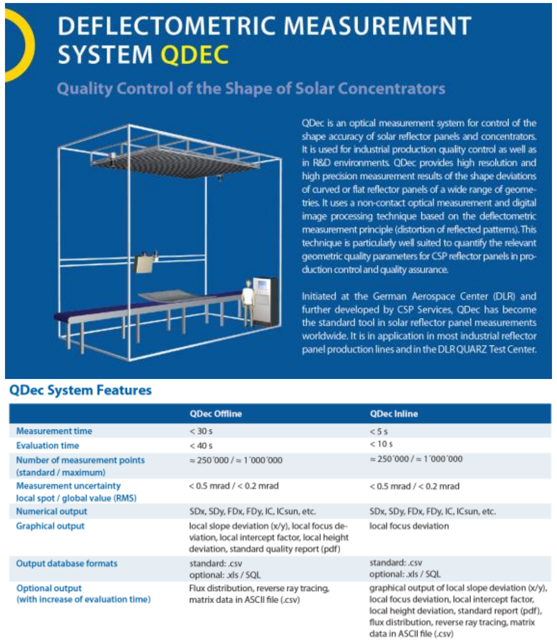

DEFLECTOMETRIC MEASUREMENT SYSTEM QDEC

Quality Control of the Shape of Solar Concentrators

QDec is an optical measurement system for control of the shape accuracy of solar reflector panels and concentrators. It is used for industrial production quality control as well as in R&D environments. QDec provides high resolution and high precision measurement results of the shape deviations of curved or flat reflector panels of a wide range of geometries. It uses a non-contact optical measurement and digital image processing technique based on the deflectometric measurement principle (distortion of reflected patterns). This technique is particularly well suited to quantify the relevant geometric quality parameters for CSP reflector panels in production control and quality assurance.

Initiated at the German Aerospace Center (DLR) and further developed by CSP Services, QDec has become the standard tool in solar reflector panel measurements worldwide. It is in application in most industrial reflector panel production lines and in the DLR QUARZ Test Center.

QDec System Features

	QDec Offline	QDec Inline
Measurement time	< 30 s	< 5 s
Evaluation time	< 40 s	< 10 s
Number of measurement points (standard / maximum)	≈ 250´000 / ≈ 1´000´000	≈ 250´000 / ≈ 1´000´000
Measurement uncertainty local spot / global value (RMS)	< 0.5 mrad / < 0.2 mrad	< 0.5 mrad / < 0.2 mrad
Numerical output	SDx, SDy, FDx, FDy, IC, ICsun, etc.	SDx, SDy, FDx, FDy, IC, ICsun, etc.
Graphical output	local slope deviation (x/y), local focus deviation, local intercept factor, local height deviation, standard quality report (pdf)	local focus deviation
Output database formats	standard: .csv optional: .xls / SQL	standard: .csv optional: .xls / SQL
Optional output (with increase of evaluation time)	Flux distribution, reverse ray tracing, matrix data in ASCII file (.csv)	graphical output of local slope deviation (x/y), local focus deviation, local intercept factor, local height deviation, standard report (pdf), flux distribution, reverse ray tracing, matrix data in ASCII file (.csv)

https://www.cspservices.de/wp-content/uploads/CSPS-QDec.pdf

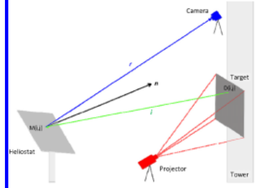

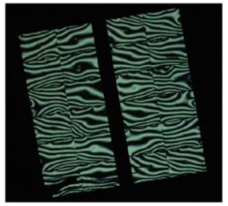

Ulmer, et al. 2014.

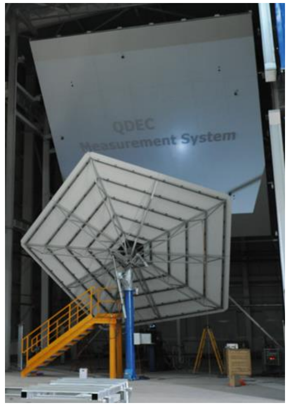

https://www.cspservices.de/quality-control/

SOFAST

Basic SOFAST Elements

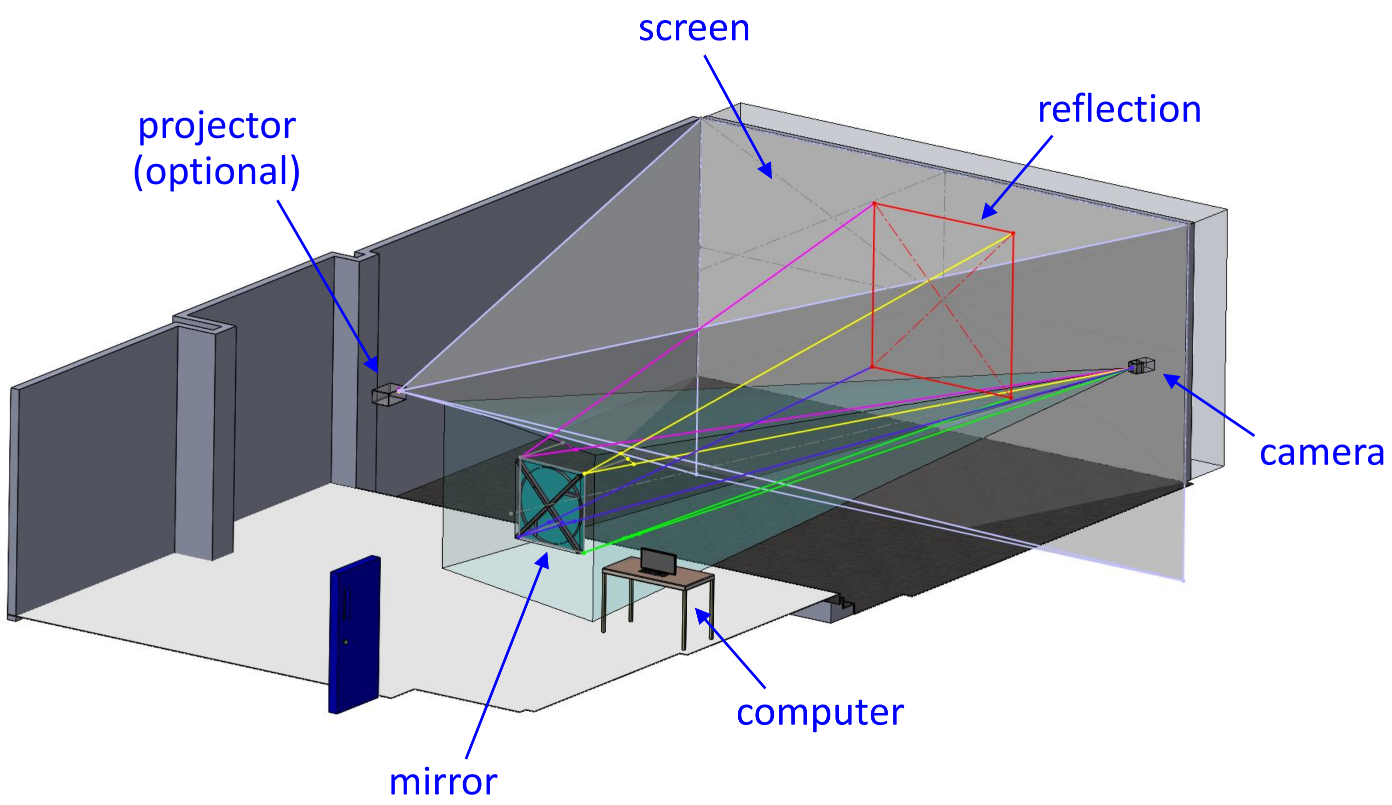

Improvements

Foundation:

- Software quality:
  - Modularity.
  - Separate data acquisition and analysis.
  - Revision control.
  - Automated test suite.
- Streamlined calibration.
- Sensitivity characterization.
- Accuracy cross-checks.

Increase value:

- New analytics.
- Flexibility.
- Measure effect of operating conditions.

Increase impact:

- Industrial support.
- Mobile SOFAST.
- Educational version.
- Easy access – open source release planned.

Green indicates work in progress.

SOFAST Configurations

Landscape
(>10 years)

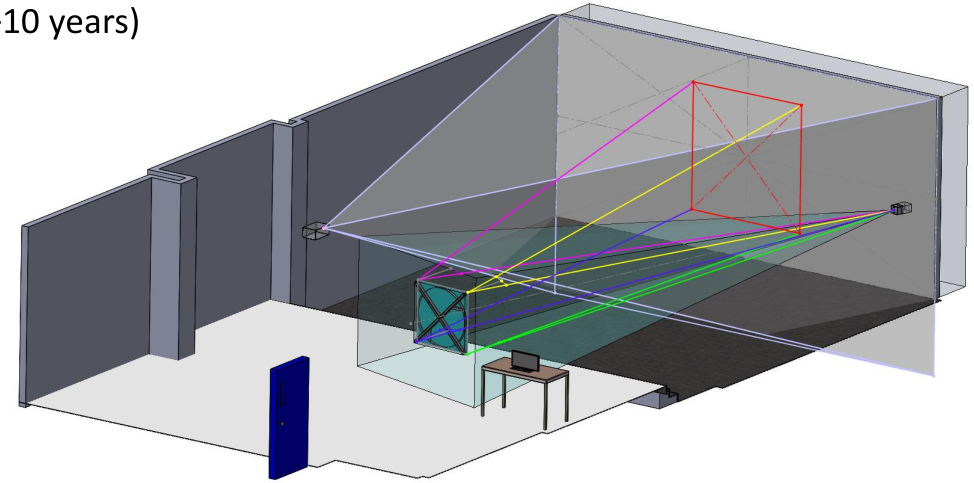

Tower*
(1 night)

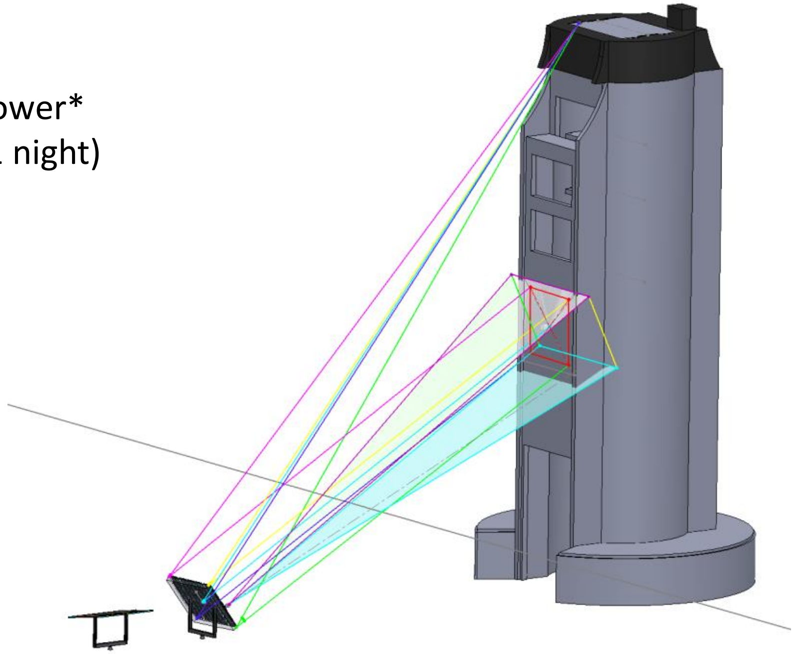

Portrait
(2 years)

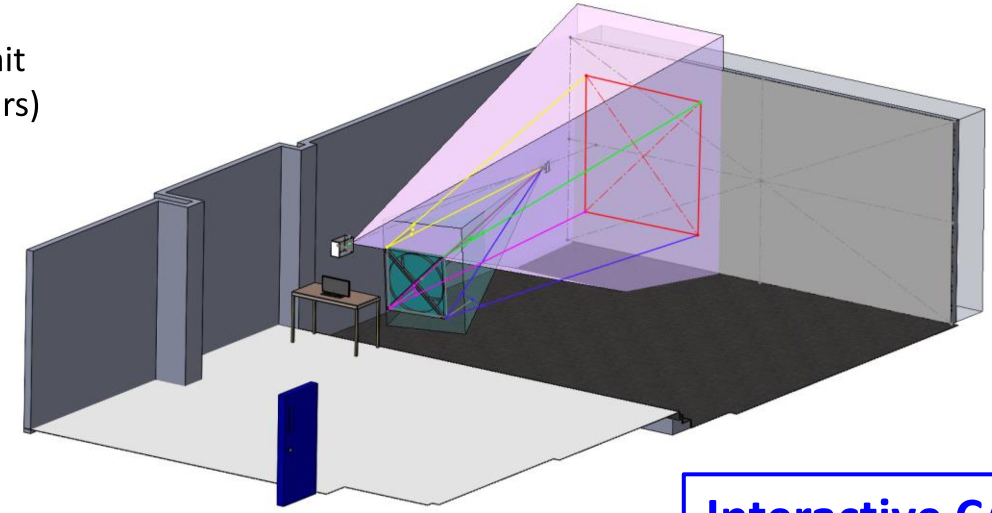

Face Up
(3 months)

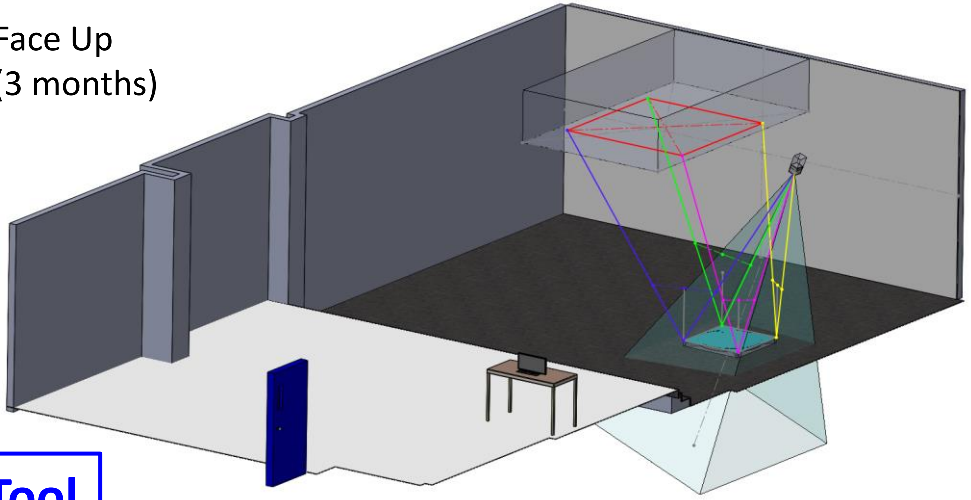

**Interactive CAD Layout Tool
(for open release)**

* Following Ulmer, et al. 2011. At Sandia, tower implementation is slow, not automated yet.

Streamlined Calibration

There are six calibration steps required for a SOFAST measurement:

Calibration steps that happen once per SOFAST installation

1) Lens Calibration

Calculates optical characteristics of the camera lens to allow following calculation:
Pixel (u, v) →pointing vector (x, y, z)

Images of a square-tiled checkerboard target are used to calculate lens focal length and tangential/radial distortion.

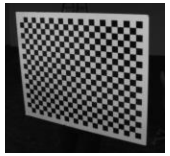

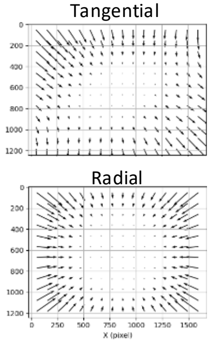

2) Projector Screen Calibration

Calculates the Z height map of the projector screen. Ray reflection calculations need the Z height of the screen.

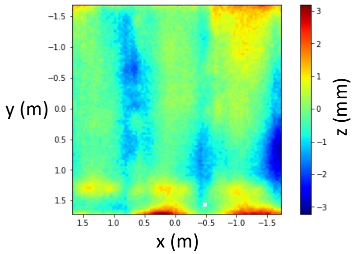

SOFAST fringes are captured with a calibrated camera (from step 1) and processed with photogrammetric algorithms.

3) Timing Calibration

Calibrates relative timing, Δt, between when a fringe image is displayed and when camera captures image. This accounts for latencies in the image display.

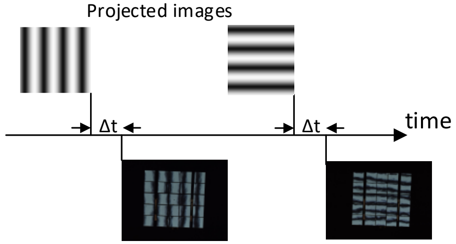

4) Screen-Camera Position Calibration

Calibrates the relative position of the screen and the camera (translation and rotation) using photogrammetry.

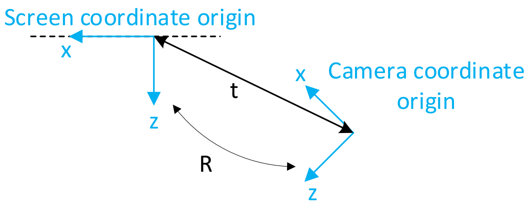

Calibration occurs every one to few SOFAST measurements

Brightness Response Calibration

SOFAST expects to capture sinusoidal fringes. Thus we need to characterize the relation between projector brightness output and camera response. The projector is sent sinusoidal fringes to display and the captured images are adjusted to account for the nonlinear response.

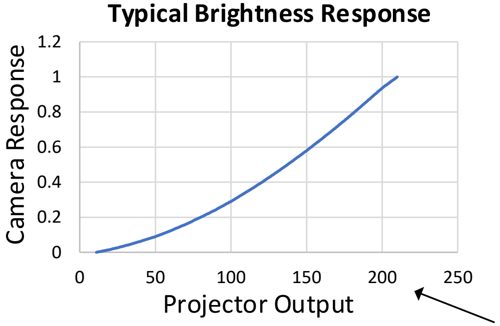

Projector brightness values are stepped from 0 to 255 for an 8-bit projector

Pose Calibration

To perform slope characterizations, SOFAST estimates the pose of the mirror using photogrammetry. SOFAST finds the corners of the mirrors algorithmically and the XYZ positions of the corners (in mirror coordinates) are user-defined. SOFAST calculates the relative pose of the mirror with respect to the camera.
We also measure the mirror-to-screen distance d_o.

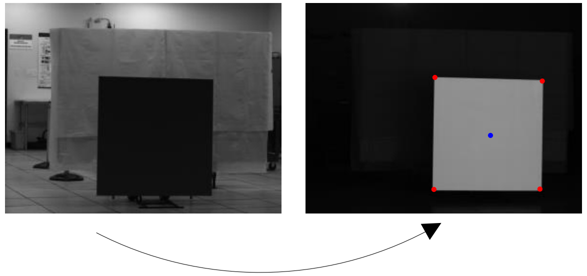

Calibration occurs during every SOFAST measurement

Data Acquisition: Example Fringe Sequence

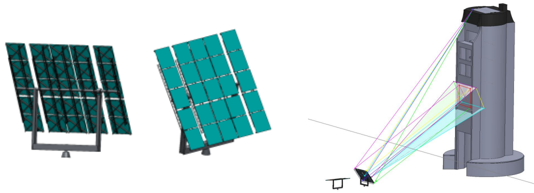

Fringe #5:

The new SOFAST separates data acquisition from data analysis.
This enables optimization of factory production cycle time, facilitates software quality control, and also greatly increases analysis flexibility.

Projected Onto Tower

Seen in Reflection

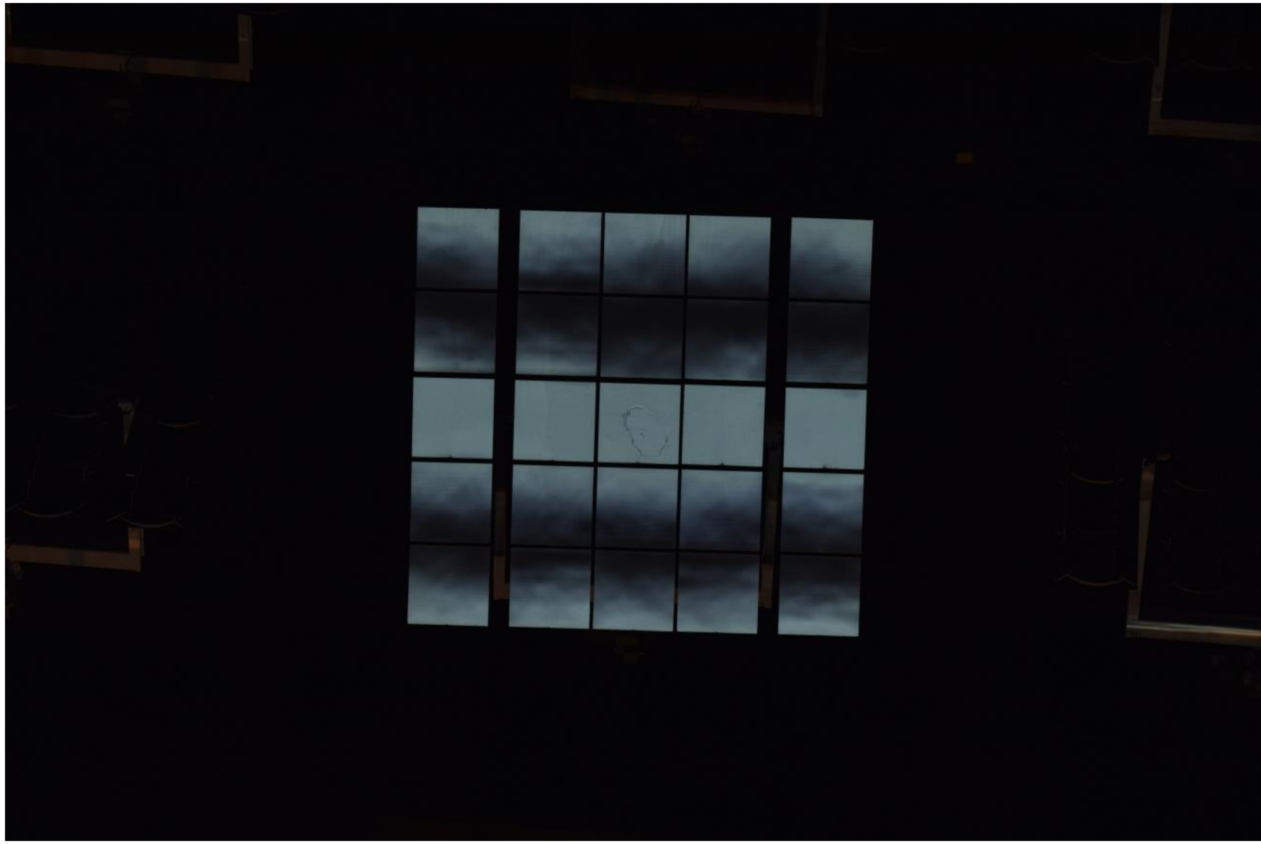

Nikon D3300, f = 107 mm

Data Acquisition: Example Fringe Sequence

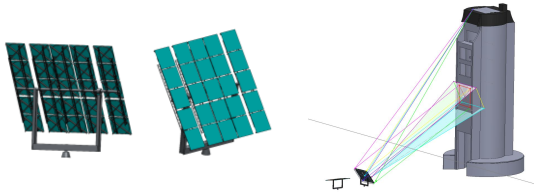

Fringe #6:

Projected Onto Tower

Seen in Reflection

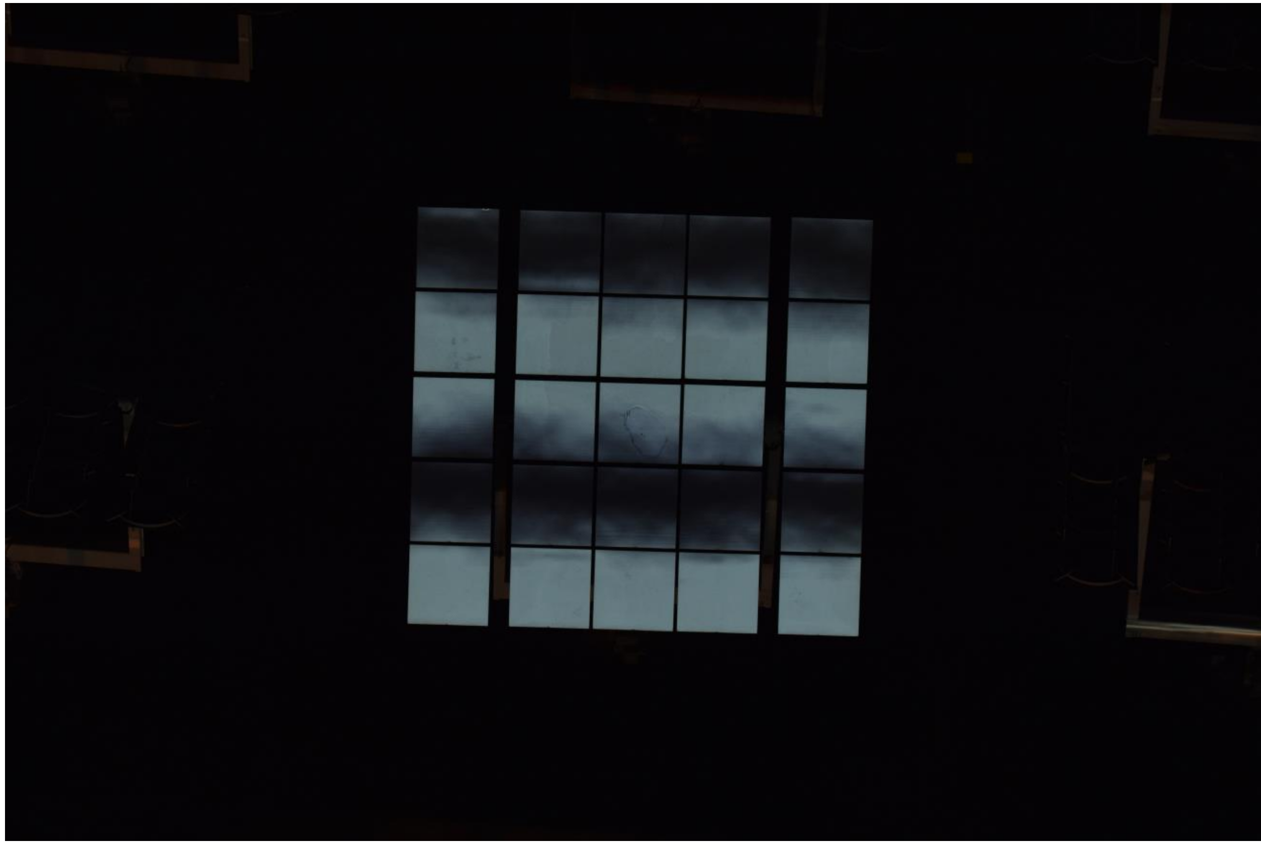

Nikon D3300, f = 107 mm

Data Acquisition: Example Fringe Sequence

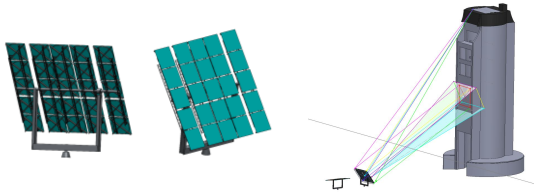

Fringe #9:

Projected Onto Tower

Seen in Reflection

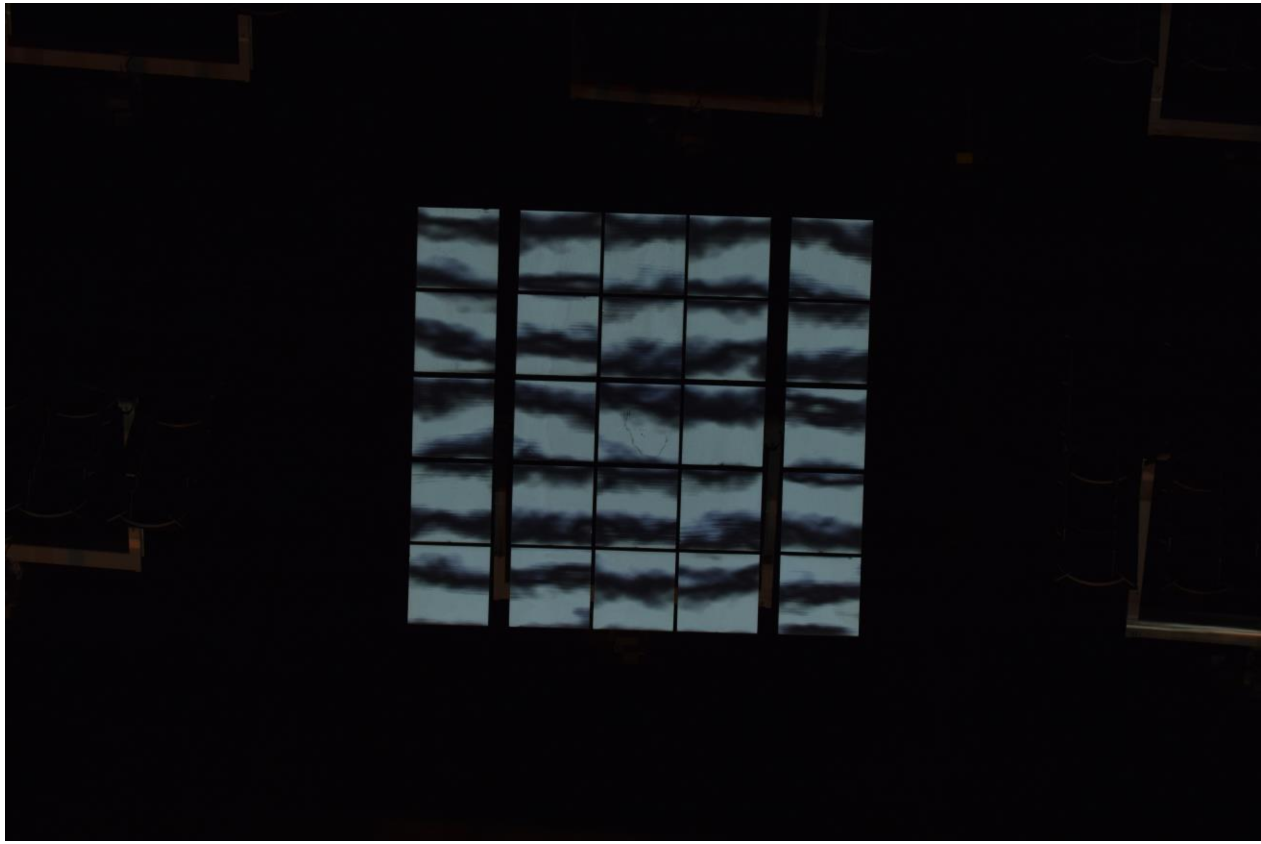

Nikon D3300, f = 107 mm

Data Acquisition: Example Fringe Sequence

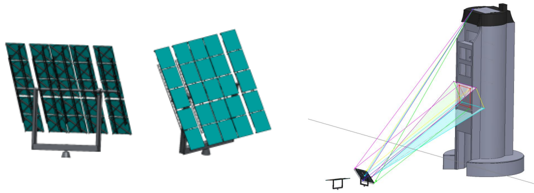

<u>Fringe #10:</u>

Projected Onto Tower

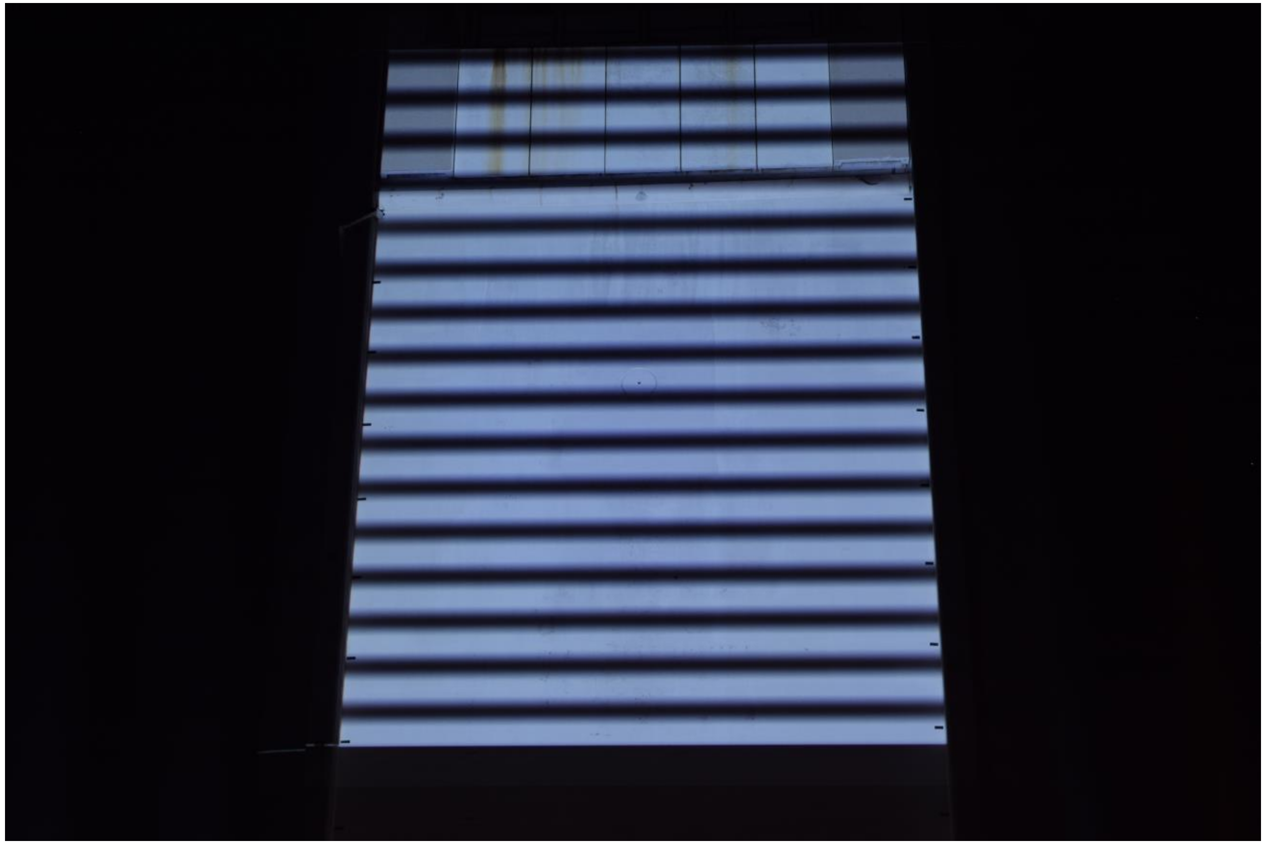

Seen in Reflection

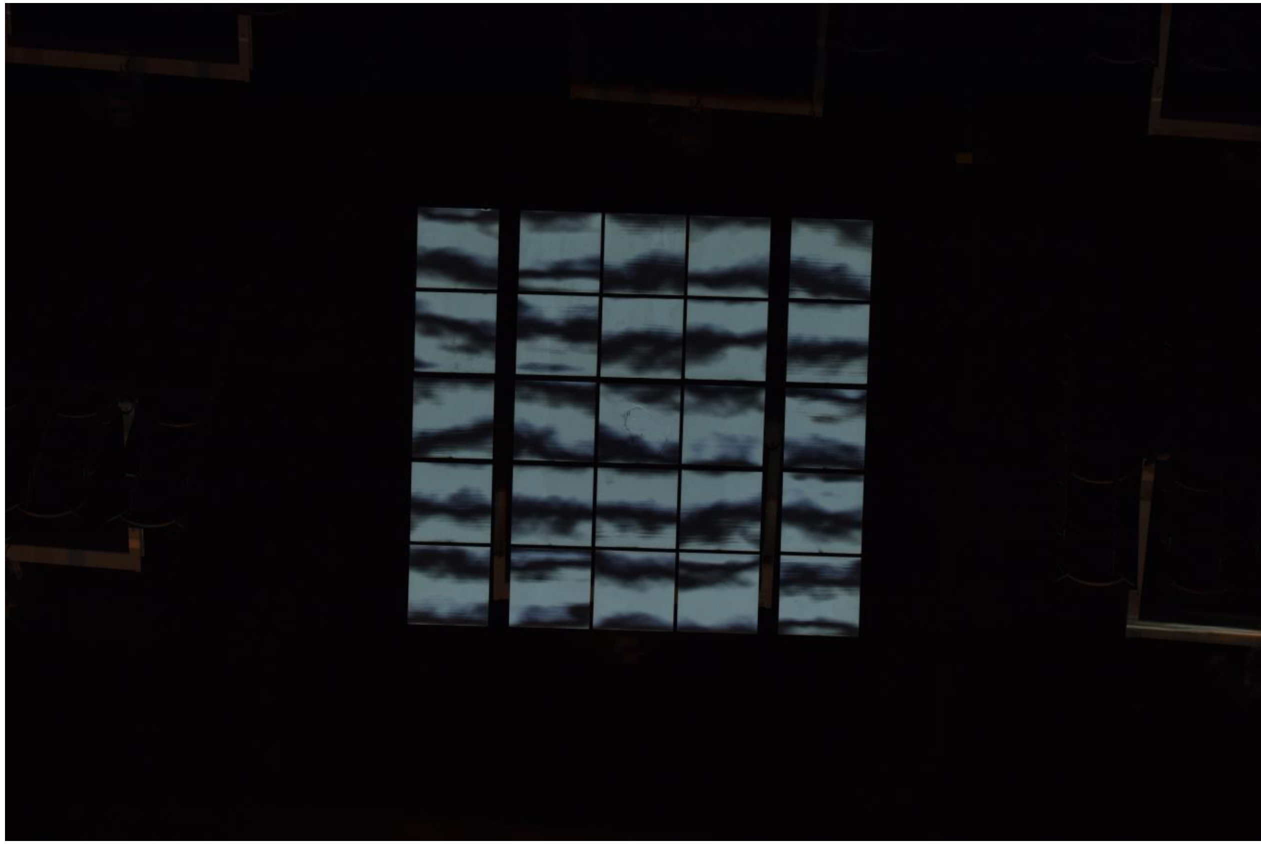

Nikon D3300, f = 107 mm

Data Acquisition: Example Fringe Sequence

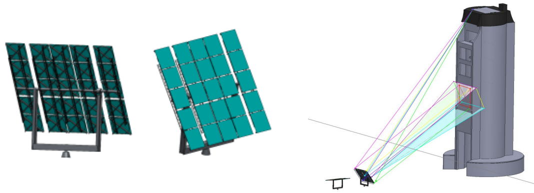

Fringe #13:

Projected Onto Tower

Seen in Reflection

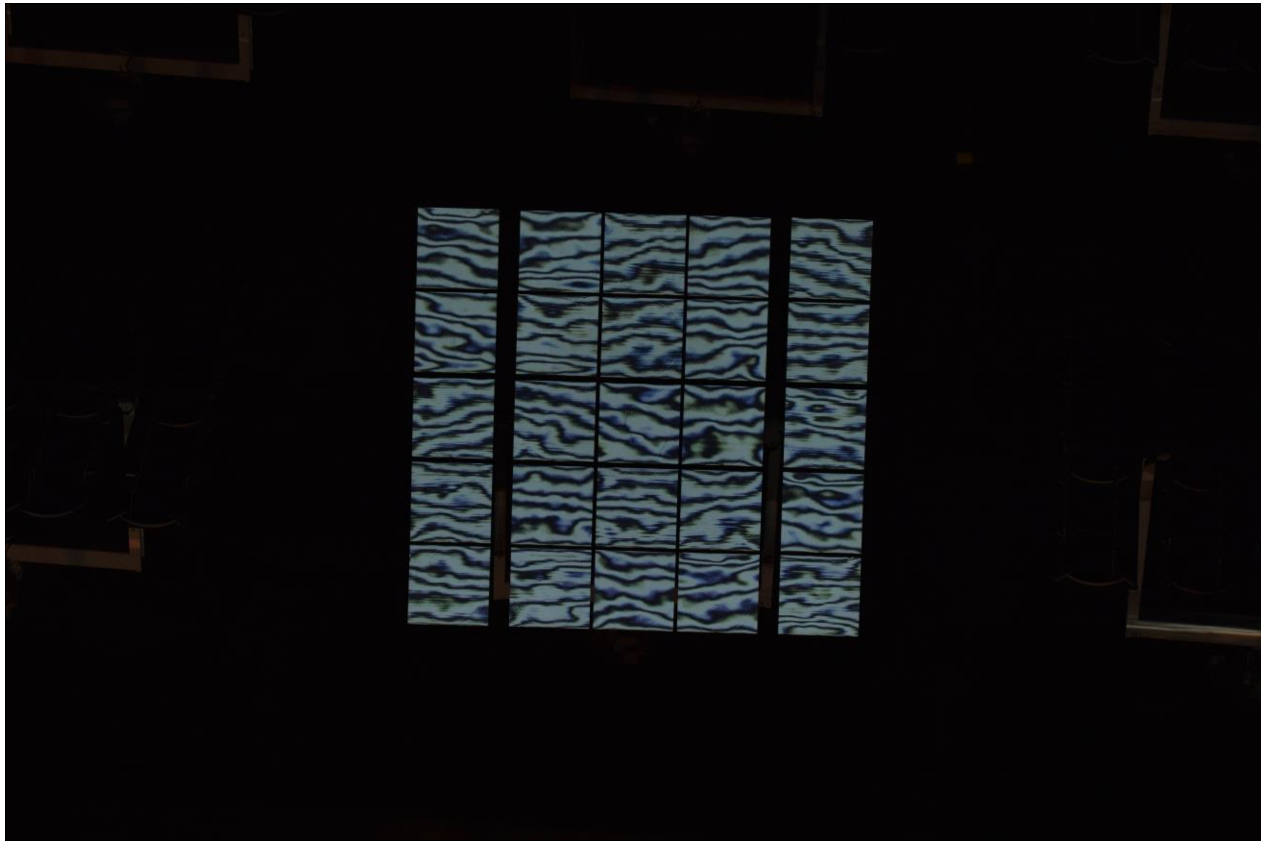

Nikon D3300, f = 107 mm

Data Acquisition: Example Fringe Sequence

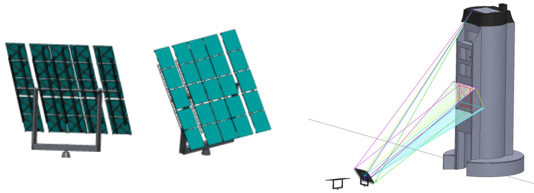

Fringe #14:

Projected Onto Tower

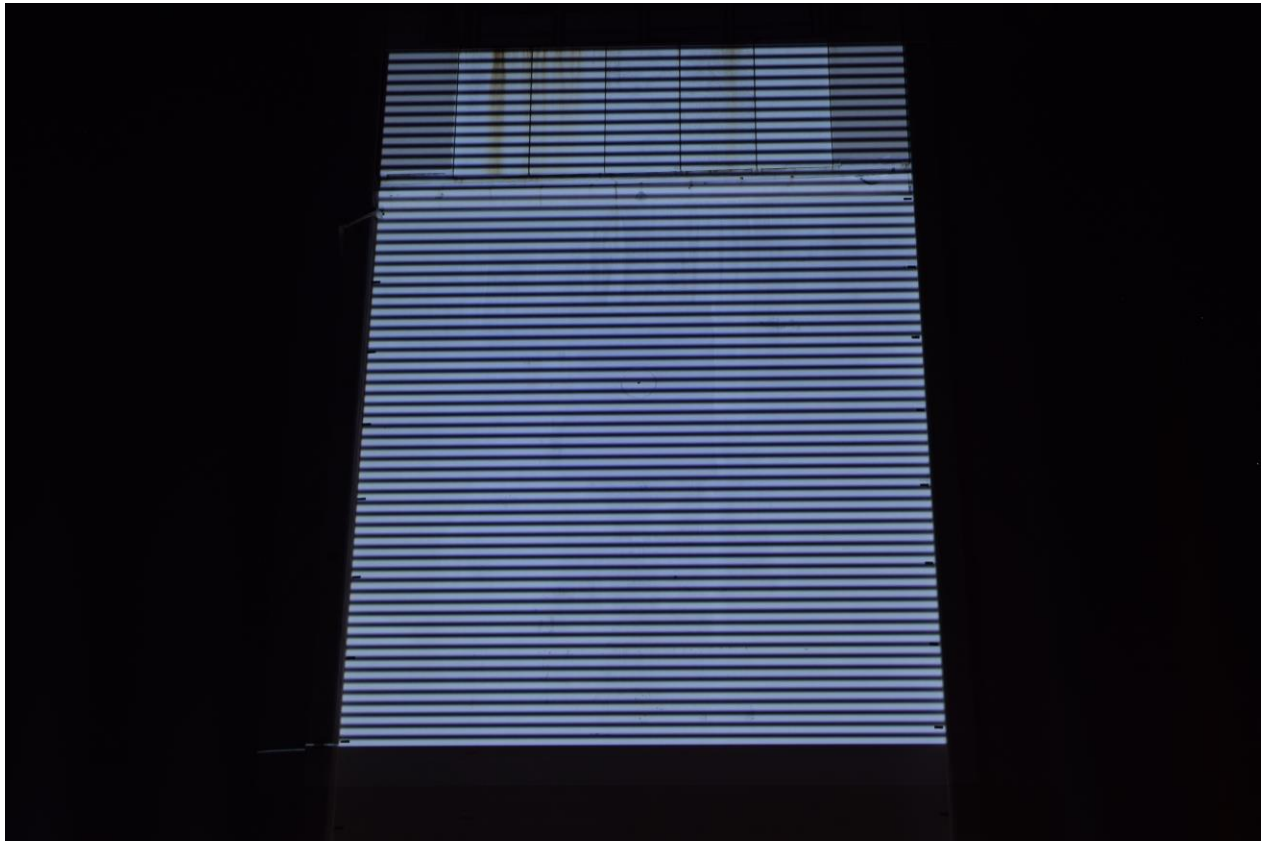

Seen in Reflection

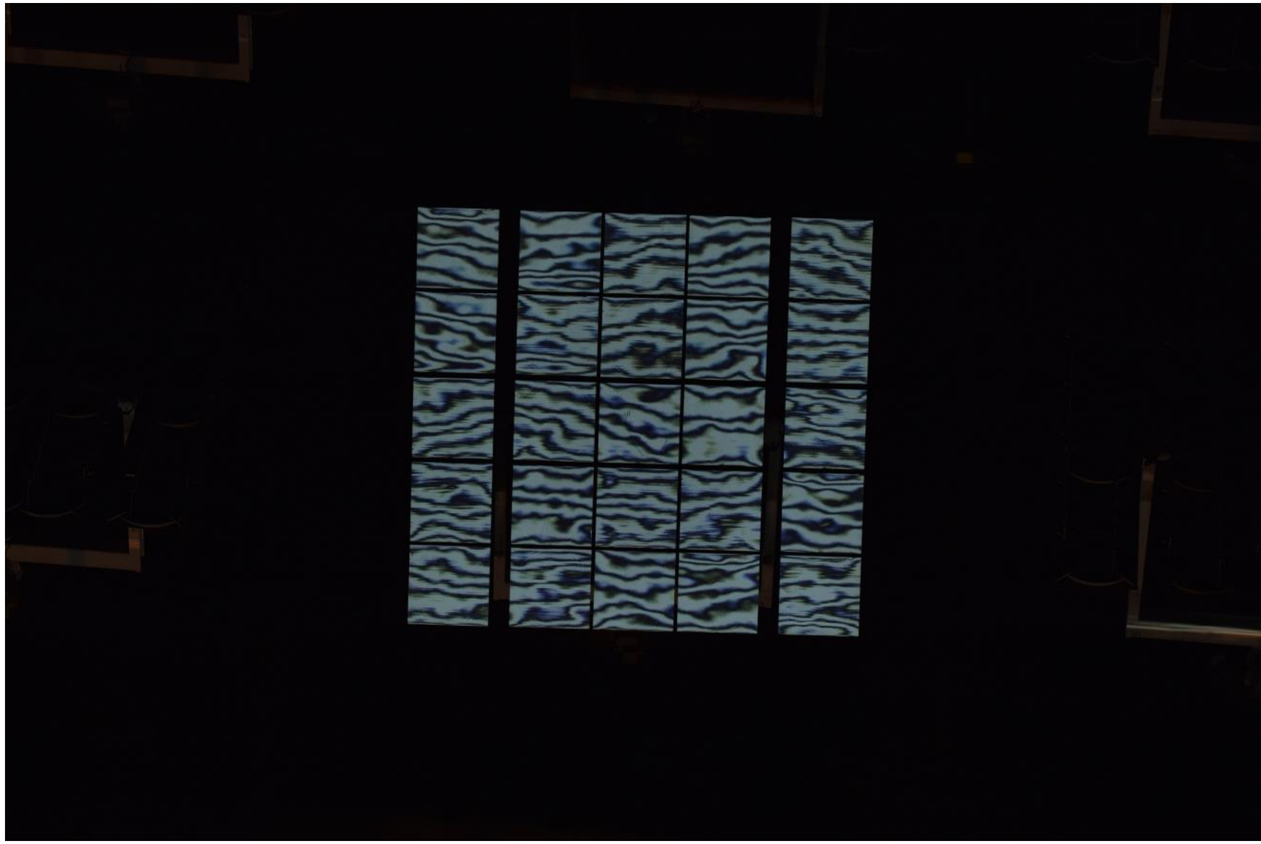

Nikon D3300, f = 107 mm

Data Acquisition: Example Fringe Sequence

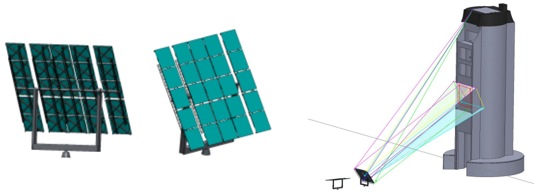

Fringe #23:

Projected Onto Tower

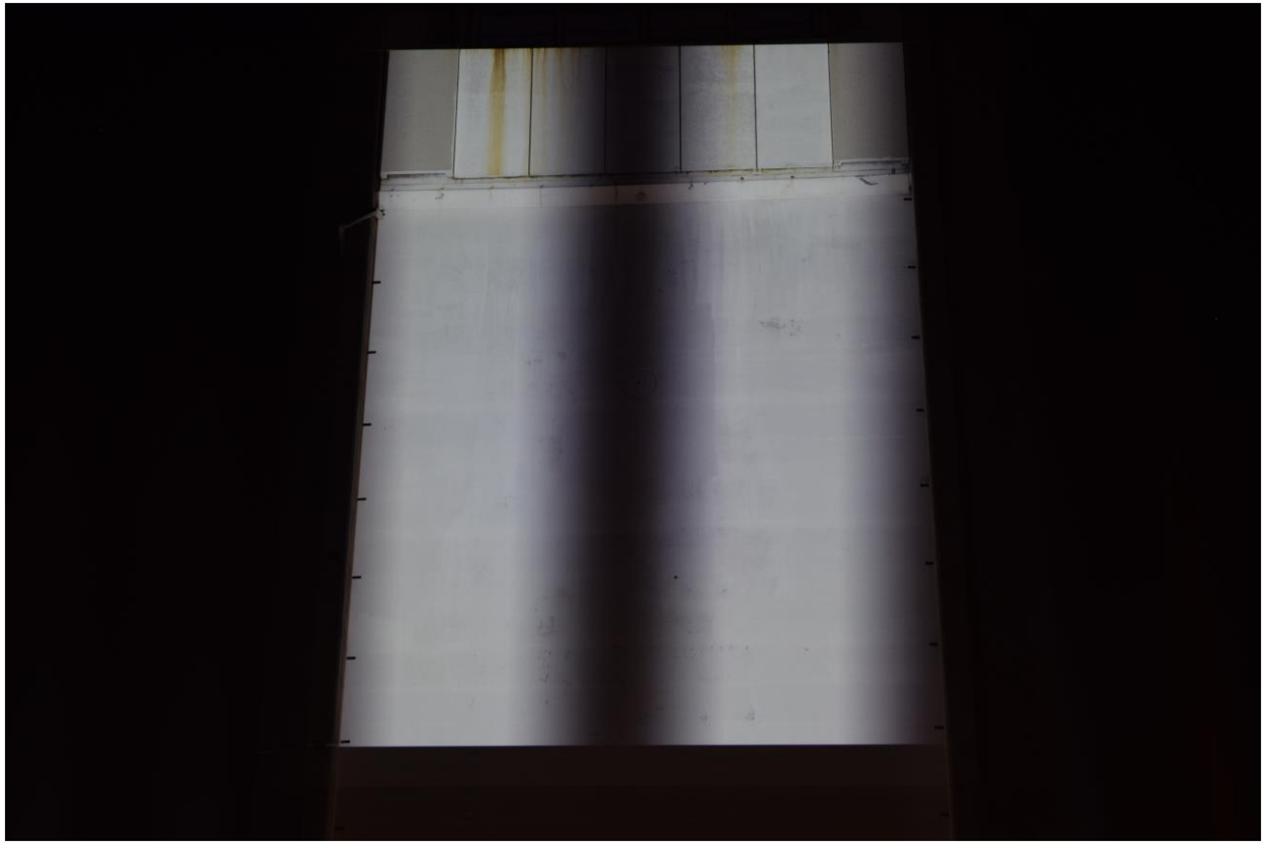

Seen in Reflection

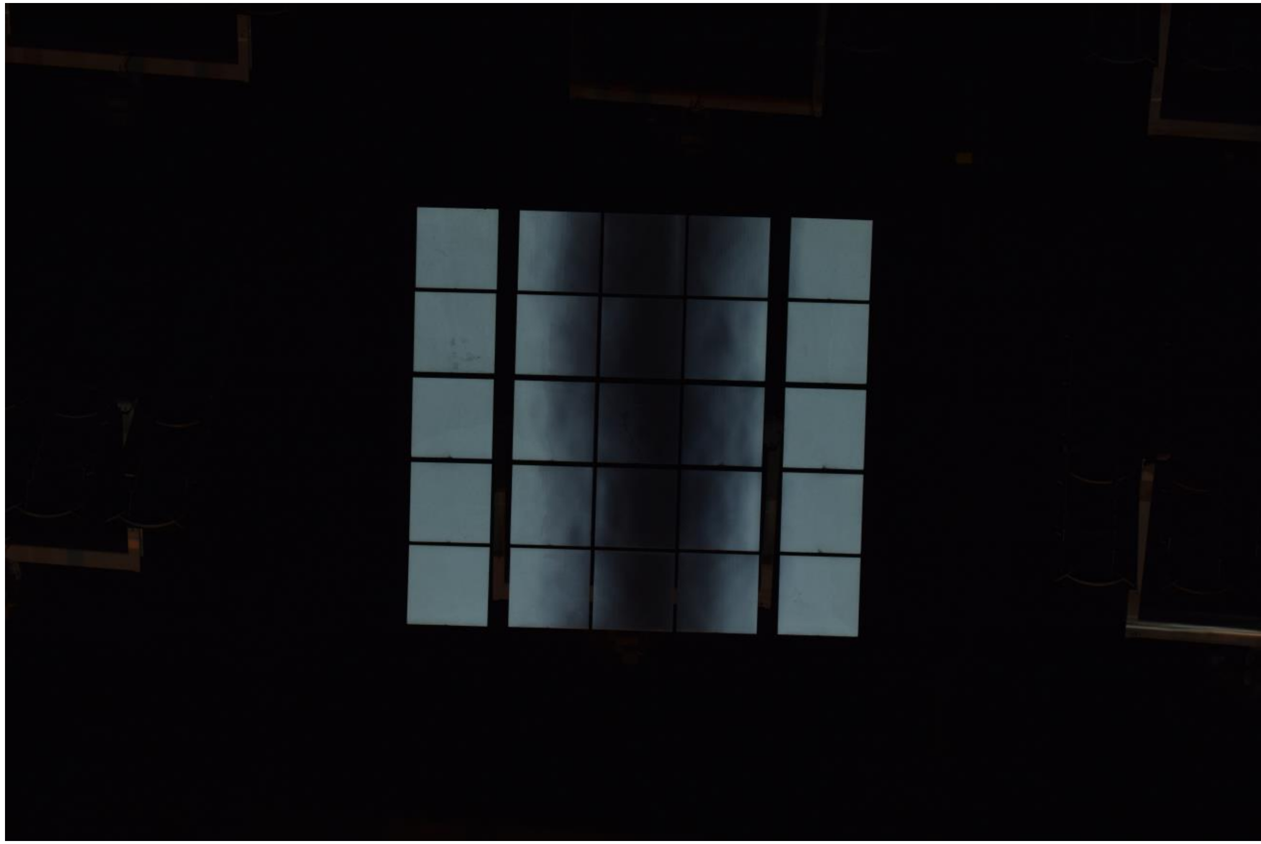

Nikon D3300, f = 107 mm

Data Acquisition: Example Fringe Sequence

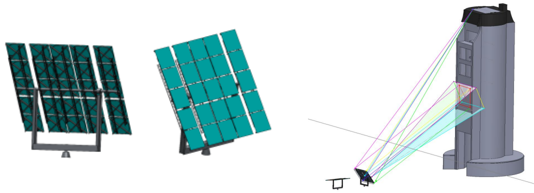

Fringe #27:

Projected Onto Tower

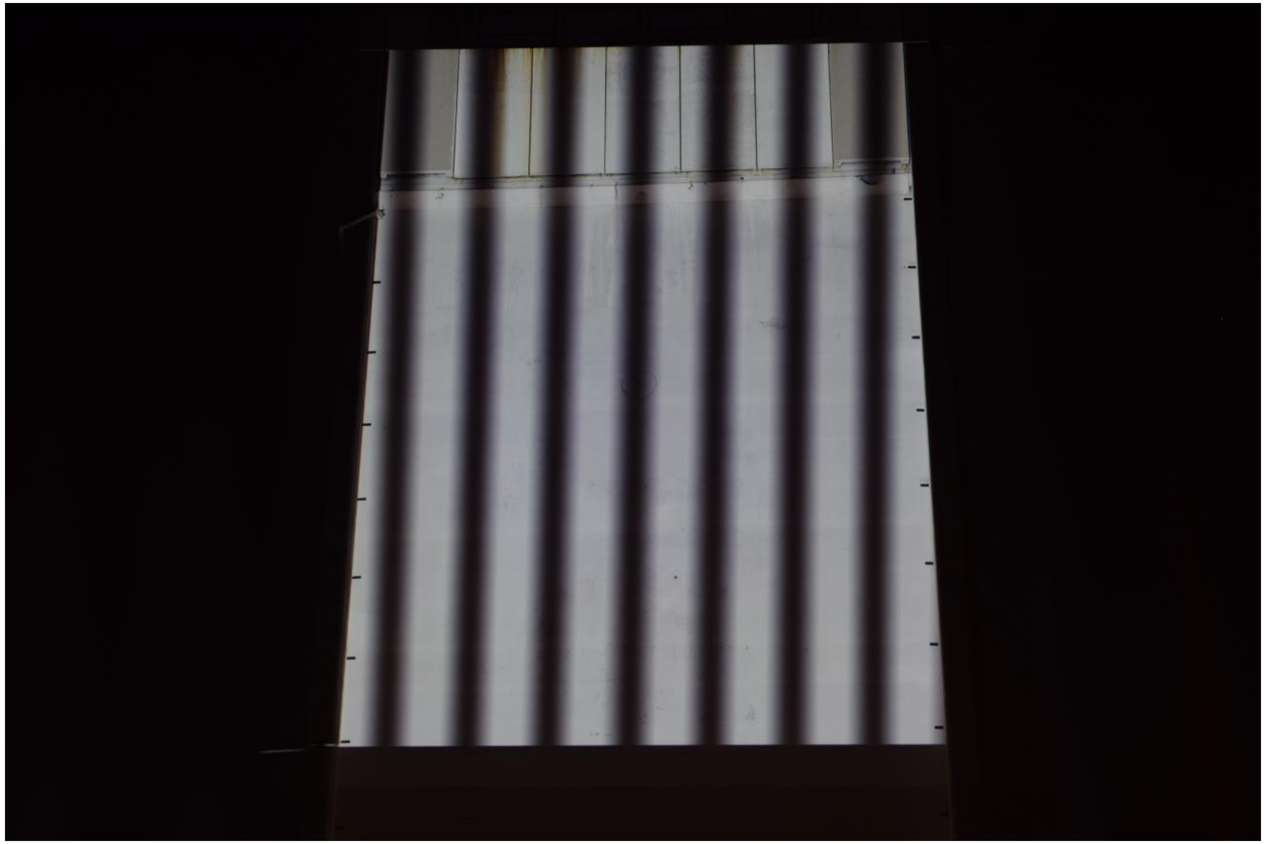

Seen in Reflection

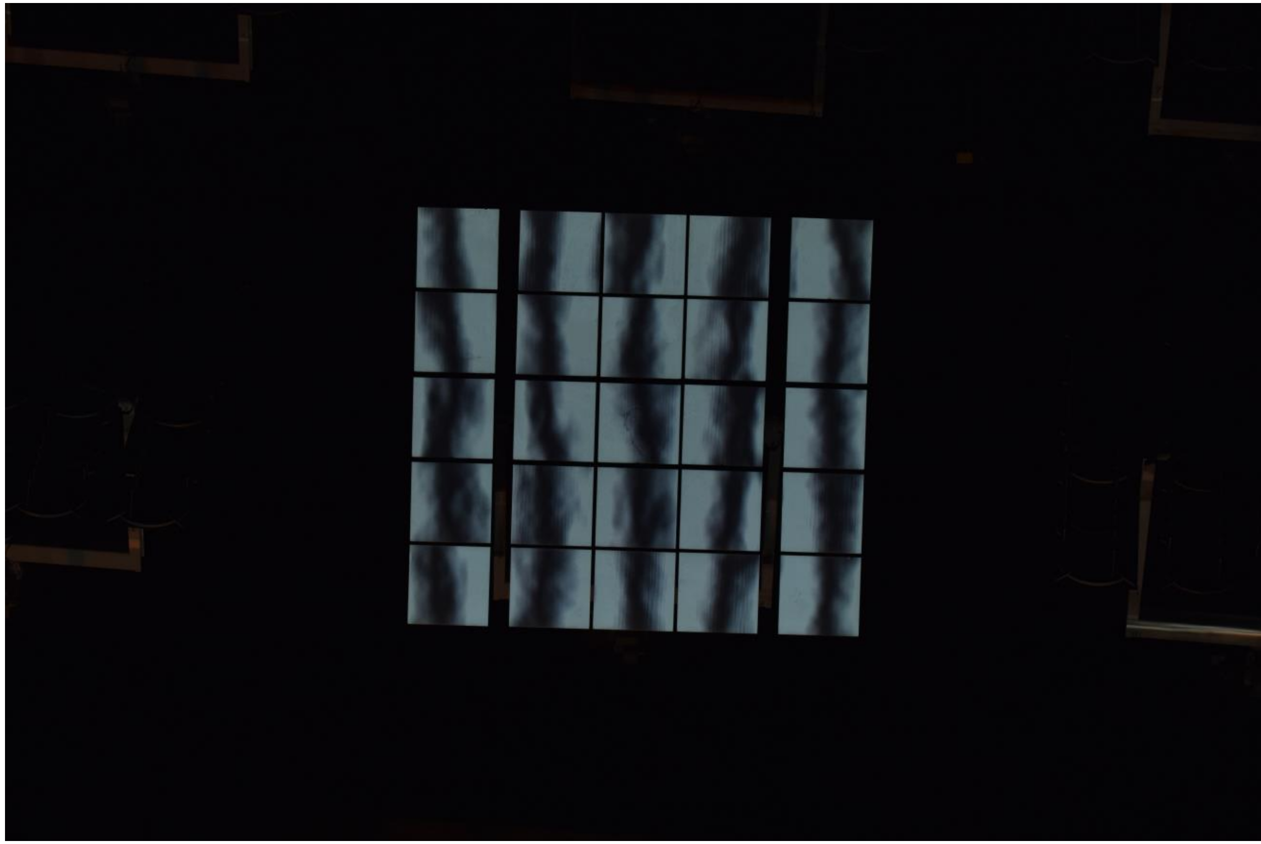

Nikon D3300, f = 107 mm

Data Acquisition: Example Fringe Sequence

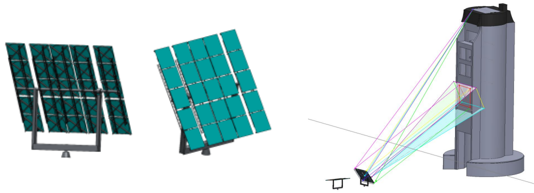

Fringe #28:

Projected Onto Tower

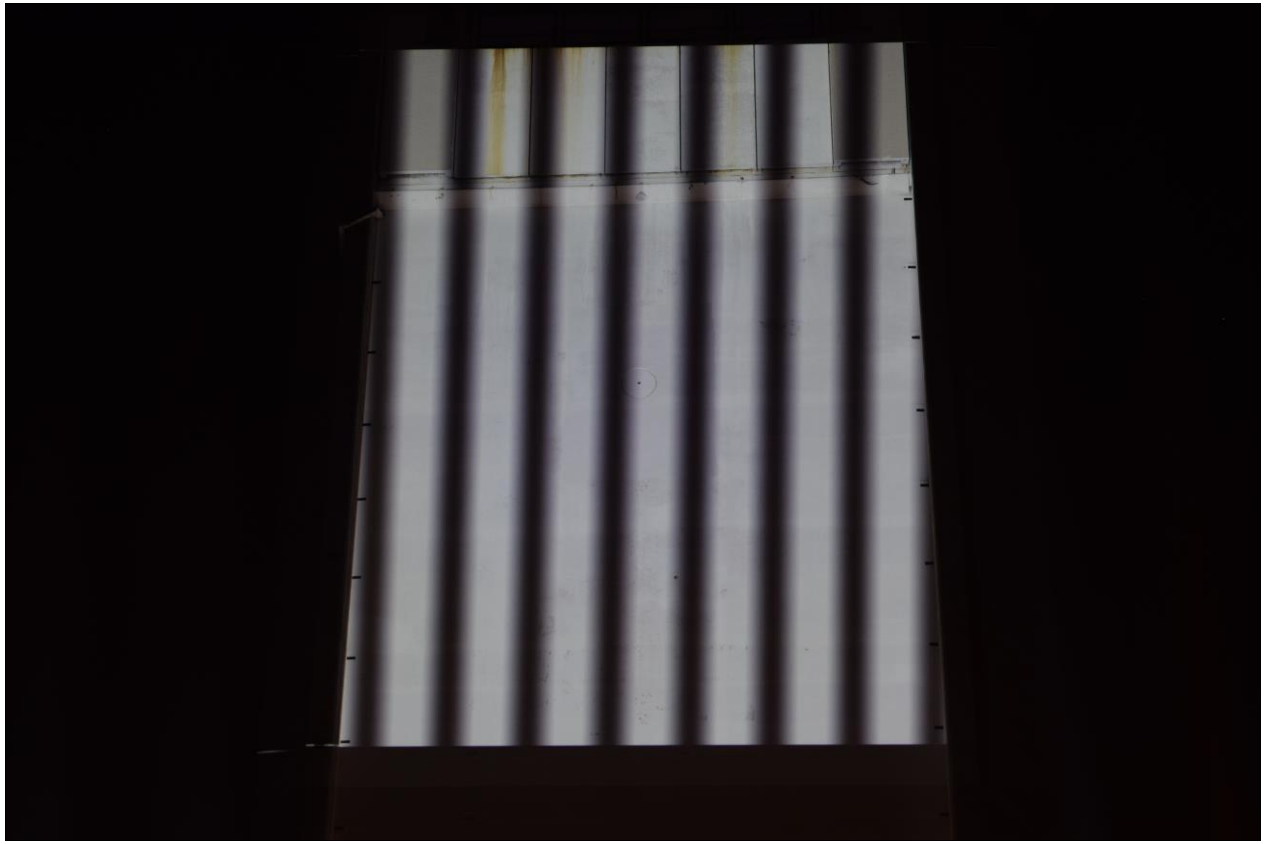

Seen in Reflection

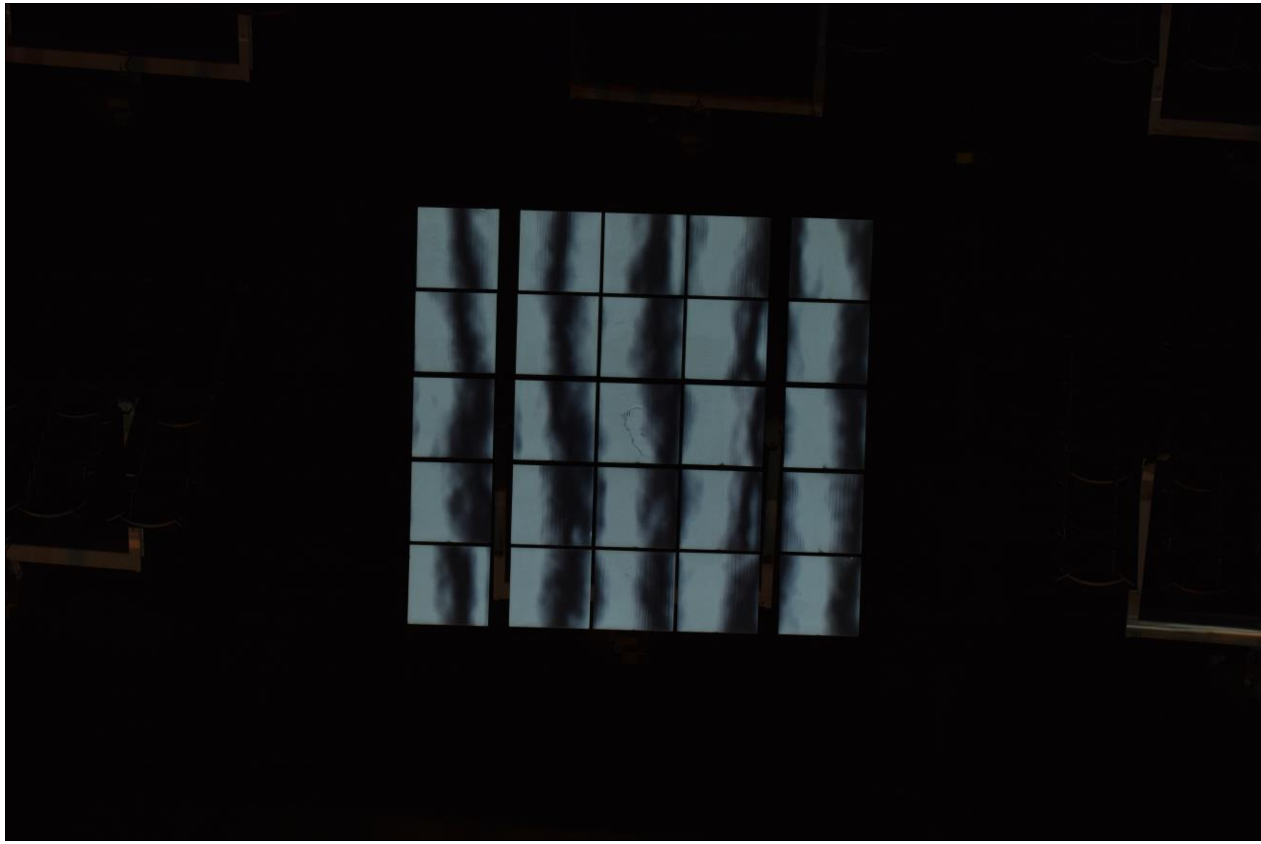

Nikon D3300, f = 107 mm

Data Acquisition: Example Fringe Sequence

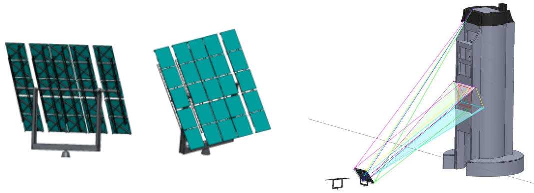

Fringe #29:

Projected Onto Tower

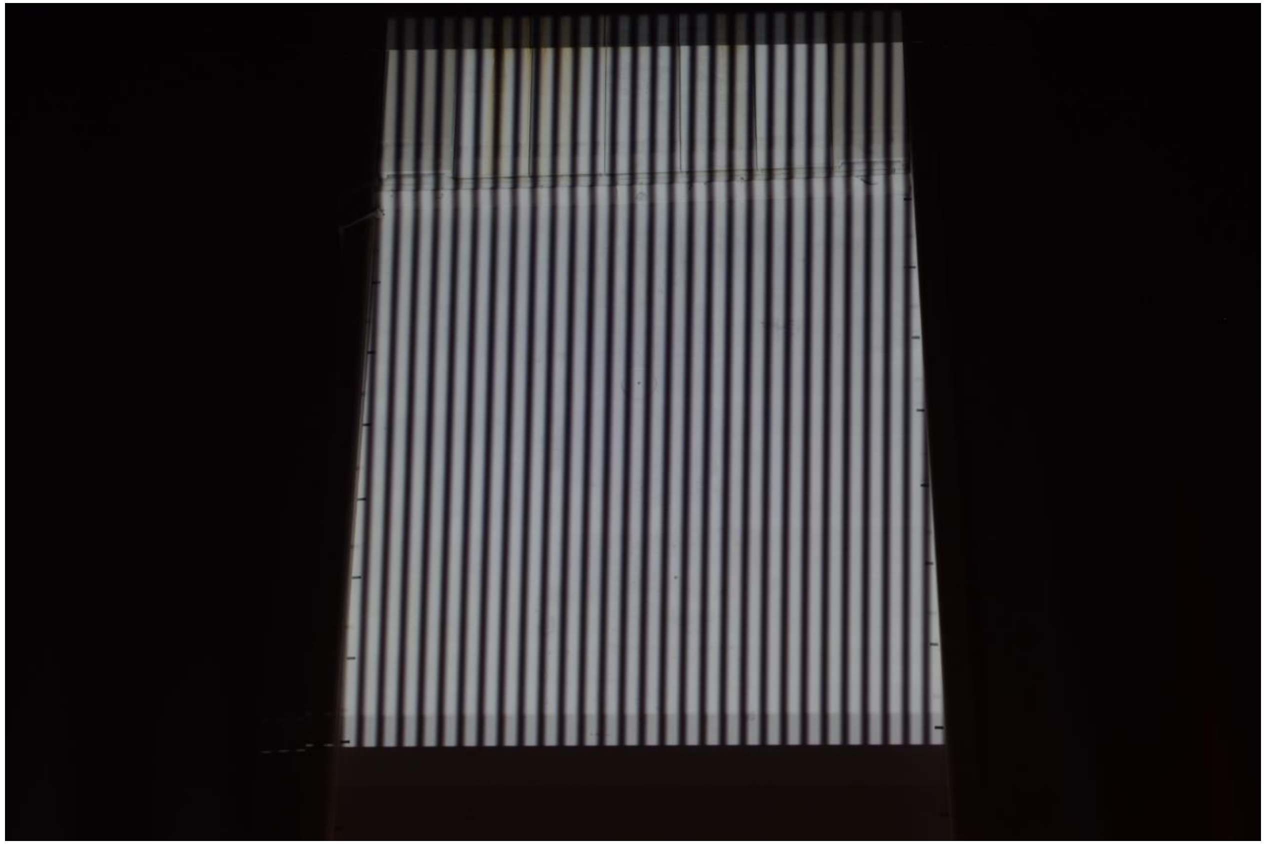

Seen in Reflection

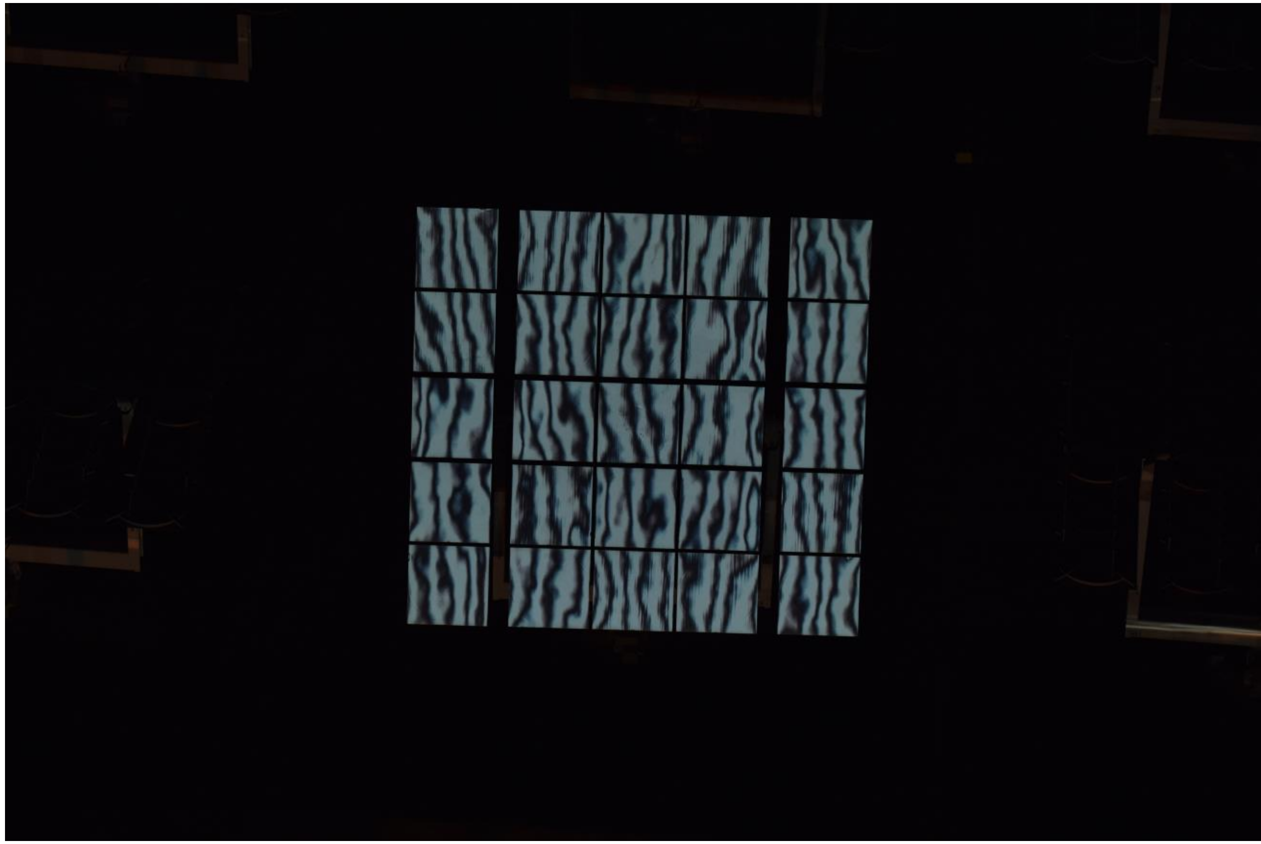

Nikon D3300, f = 107 mm

Computation 1: Primary Slope

A. Fringe intensity adjustment.

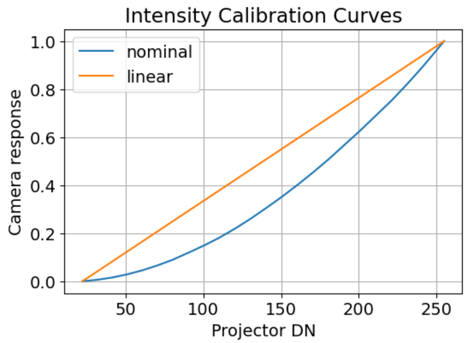

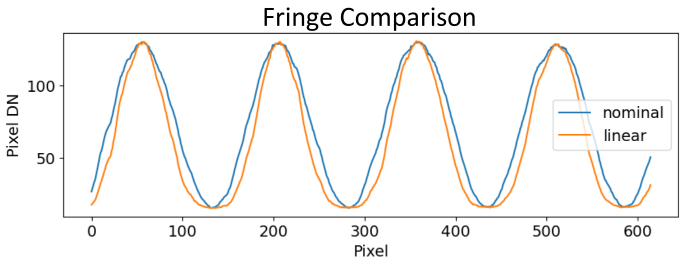

B. Mirror-to-screen point correspondence.

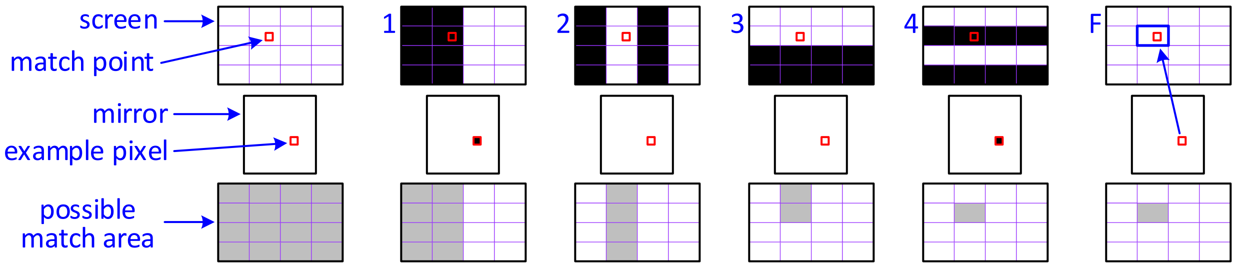

C. Surface slope estimation.

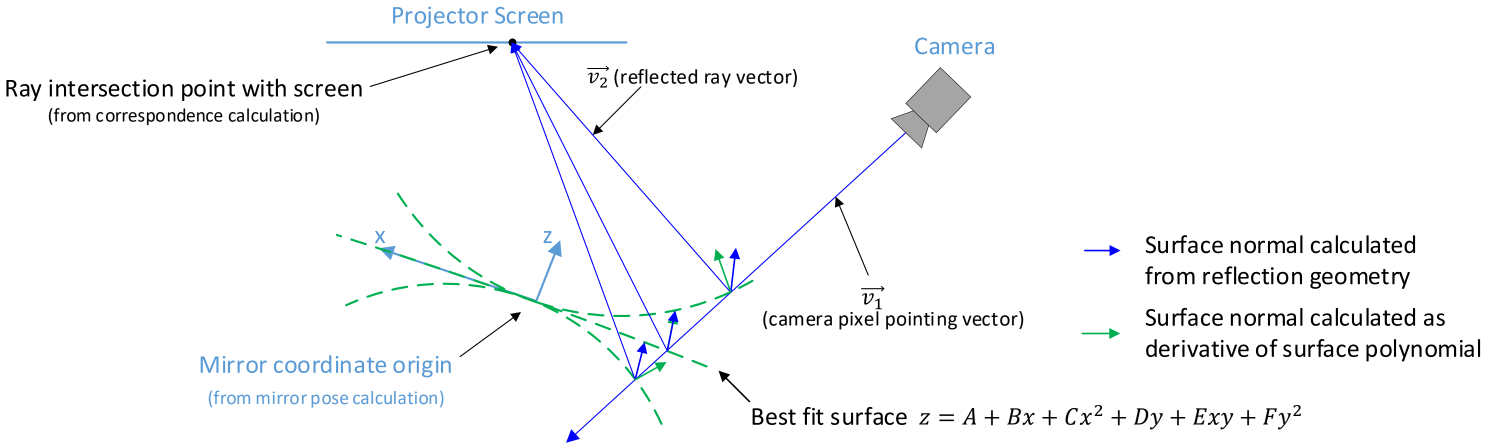

Result:

Measured X Slope

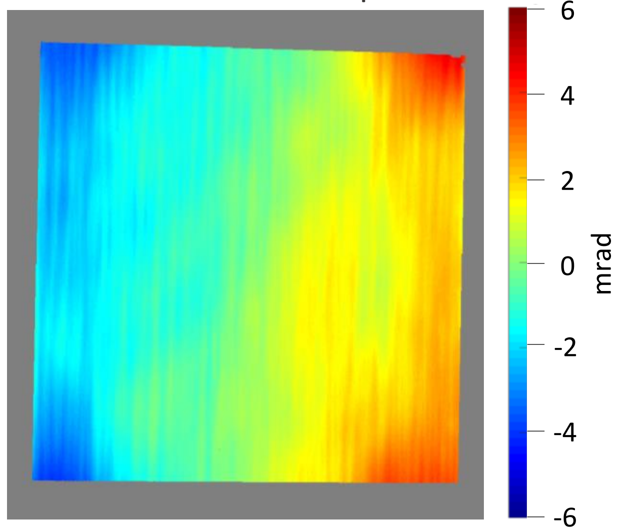

Measured Y Slope

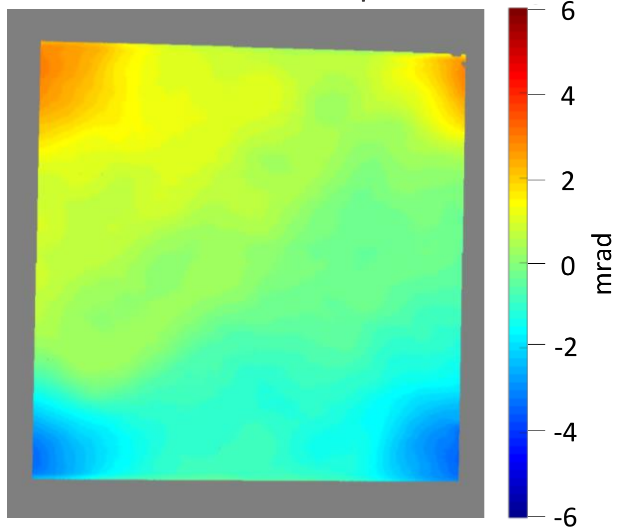

Computation 2: Slope Analysis

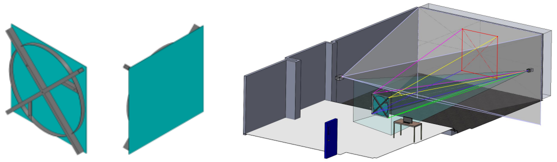

Direct: Slope Components

Measured X Slope

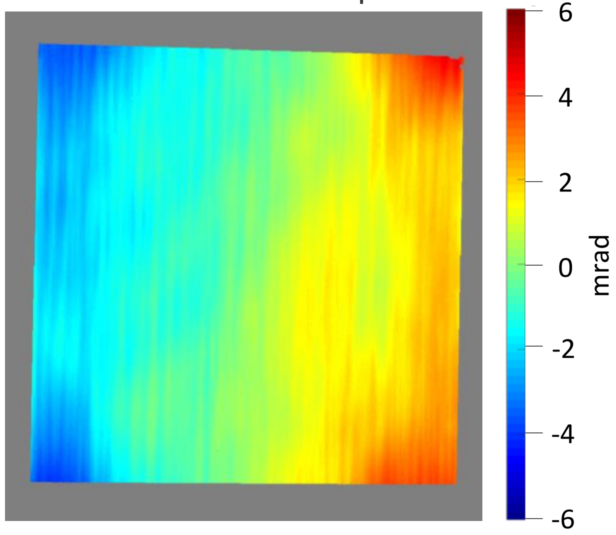

Measured Y Slope

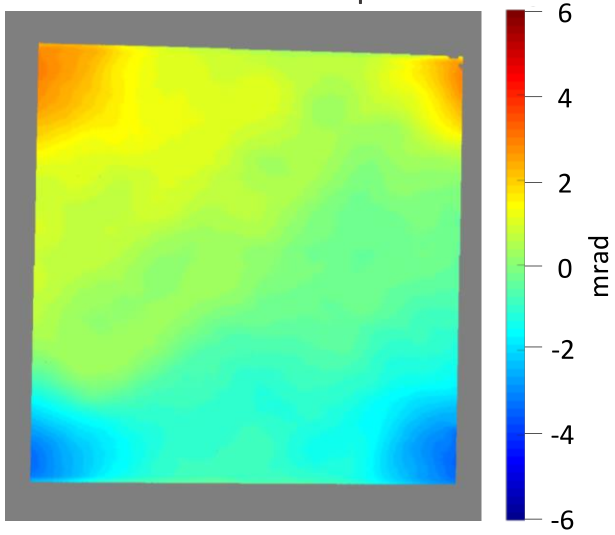

Derived: Slope Magnitude

Measured Slope Magnitude

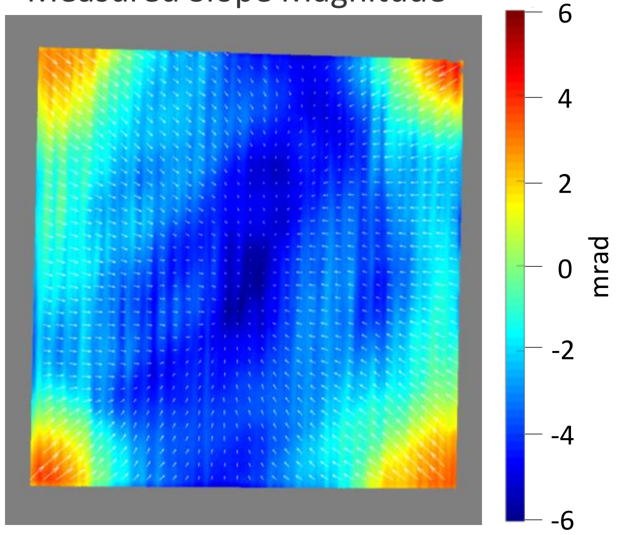

Derived: Measurement Details

Mirror:	NSTTF Facet N-001
Instrument:	SOFAST Landscape
Date/time:	2022-07-28 12:01
Sample points:	Grid
Number points:	450,000
Resolution X:	1.9 mm/pt
Resolution Y:	1.8 mm/pt
Uncertainty:	±TBD mrad

Derived: Curvature

Measured X Curvature

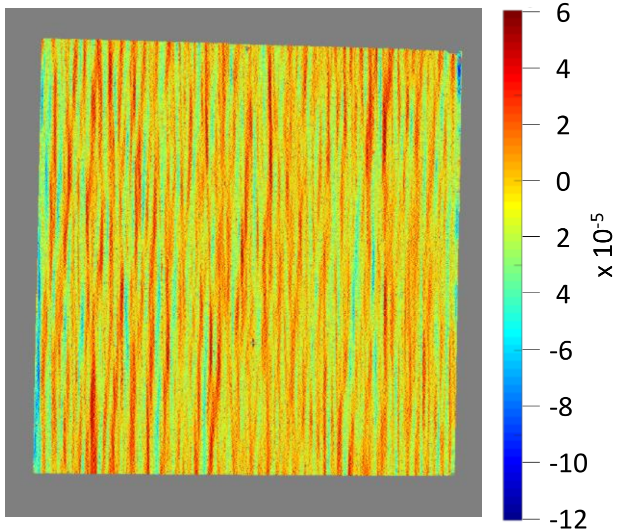

Measured Y Curvature

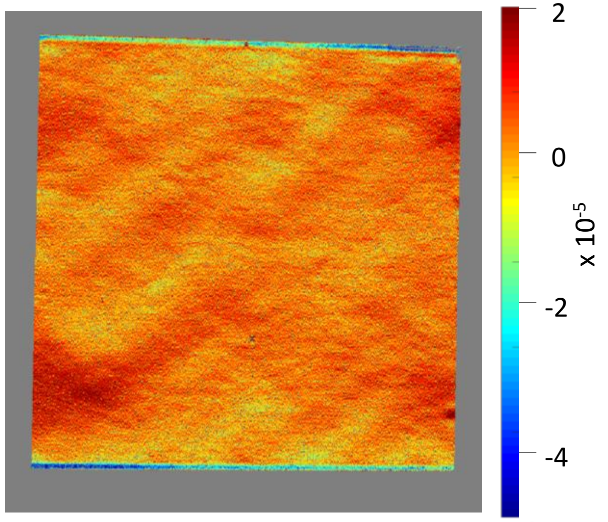

Computation 3: Error Analysis

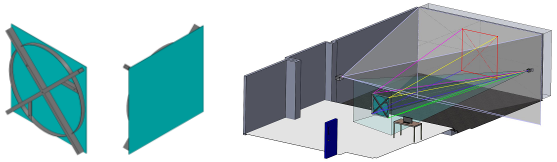

New Information

Additional information:

Ideal Design

$$z = \frac{x^2}{4f_x} + \frac{y^2}{4f_y}$$

$f_x = 100$ m

$f_y = 100$ m

$l_x = 1.22$ m

$l_y = 1.22$ m

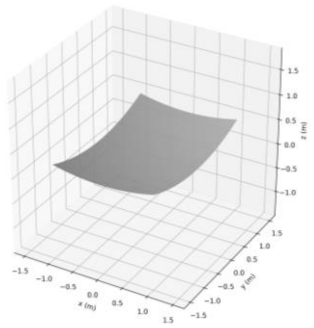

Measured X Slope

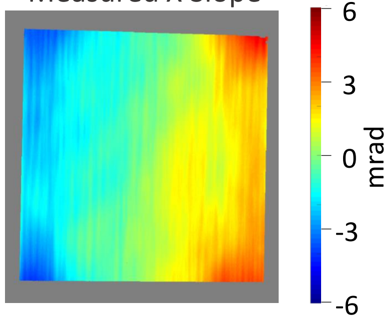

Measured Y Slope

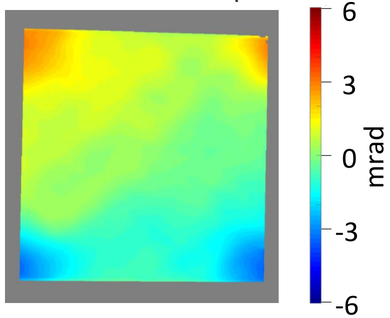

Ideal X Slope

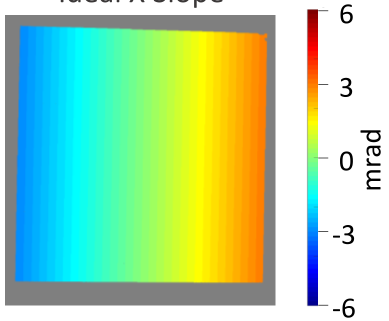

Ideal Y Slope

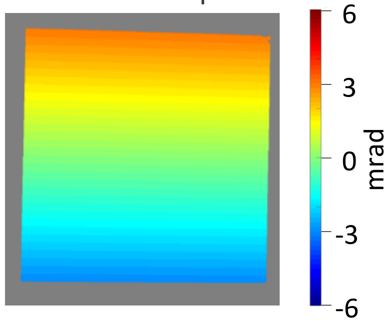

X Slope Error

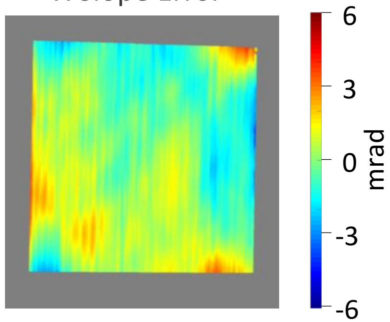

Y Slope Error

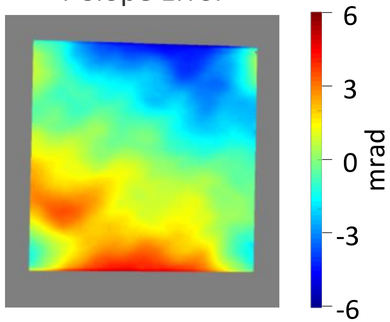

Slope Error Magnitude

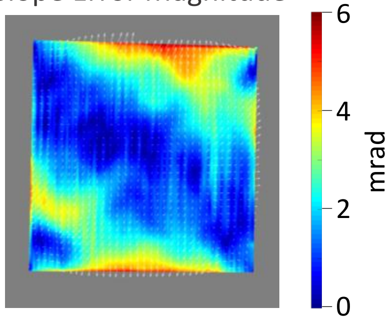

Error Statistics

RMS magnitude:	1.10 mrad
RMS error X:	0.51 mrad
RMS error Y:	0.97 mrad
⋮	⋮

Ray Trace Analysis

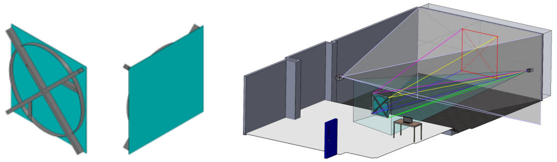

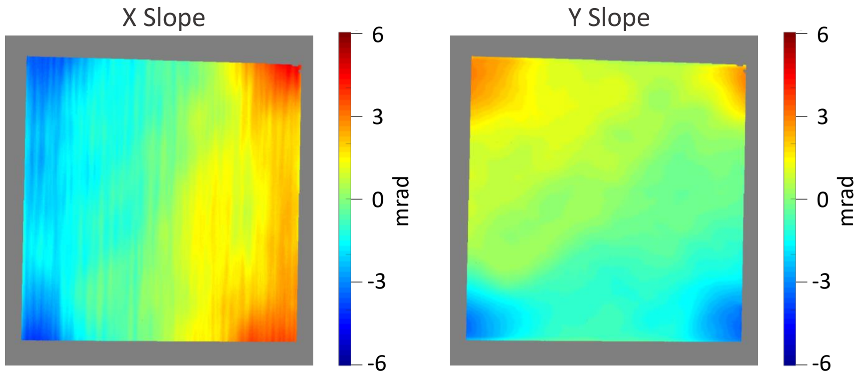

+

Parallel Rays
Target at
Focal Point

Ray Trace

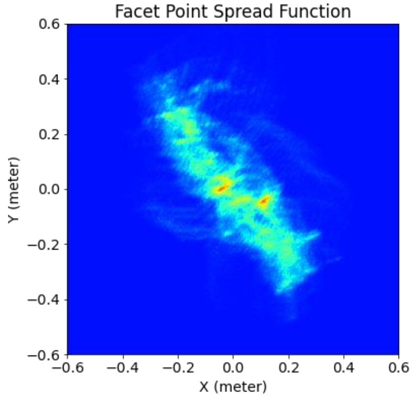

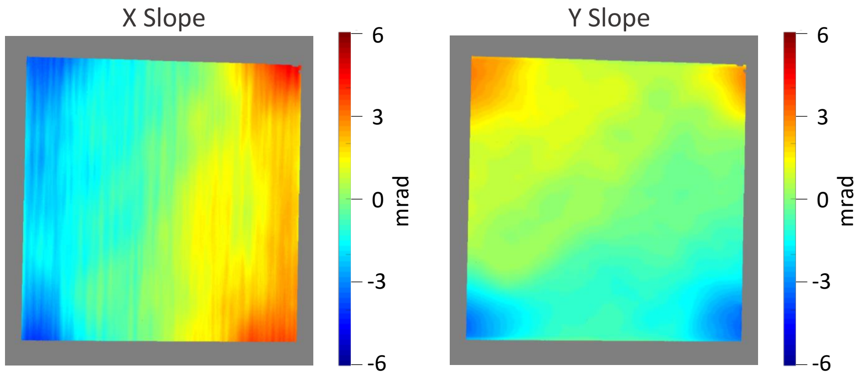

+

Desired 2f
Distance
(See below)

Ray Trace

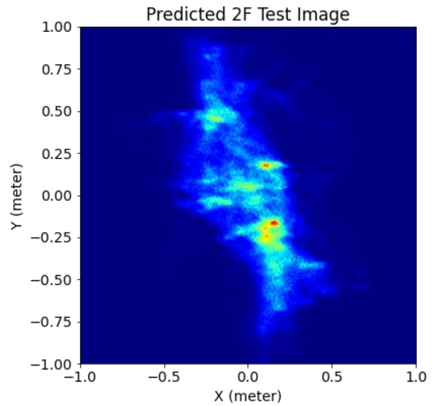

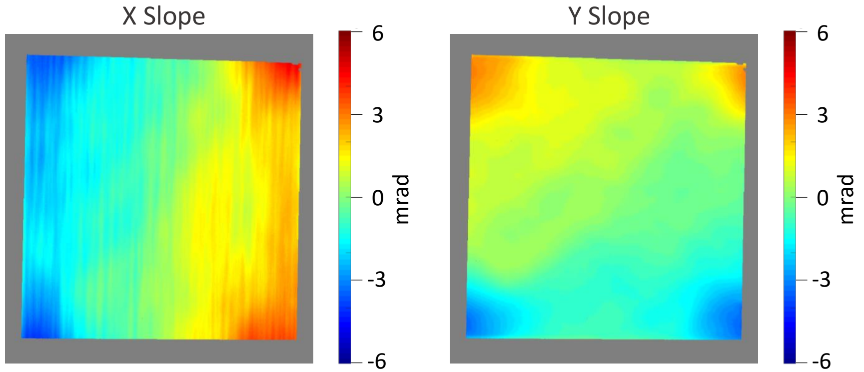

+

<u>Input:</u>
- Location in Field
- Target Location
- Where on Earth
- Date and Time

Ray Trace

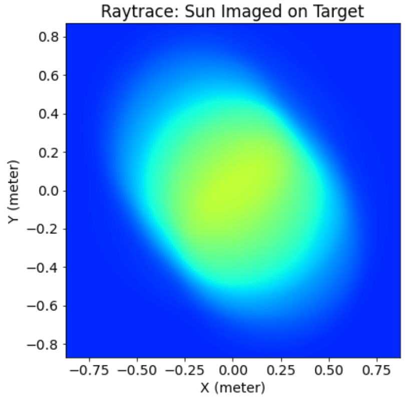

Output Summary: NSTTF Facet

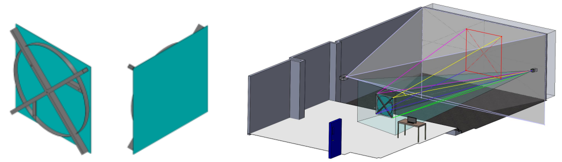

Absolute

Input: Measurement

Mirror:	NSTTF Facet N-001
Instrument:	SOFAST Landscape
Date/time:	2022-07-28 12:01
Sample points:	Grid
Number points:	452,000
Resolution X:	1.9 mm/pt
Resolution Y:	1.8 mm/pt
Uncertainty:	±TBD mrad

Slope Magnitude

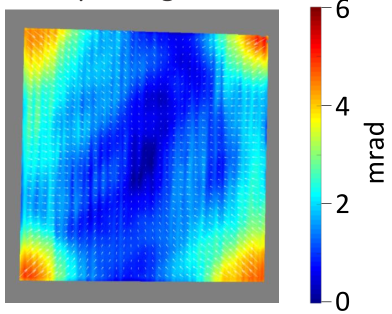

X Slope

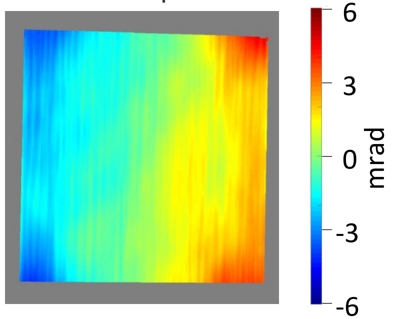

Y Slope

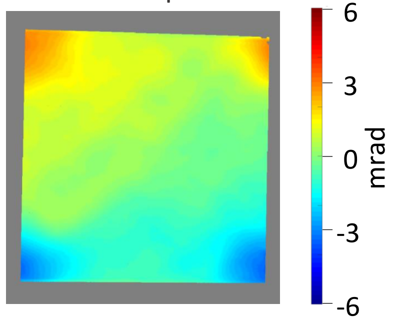

X Curvature

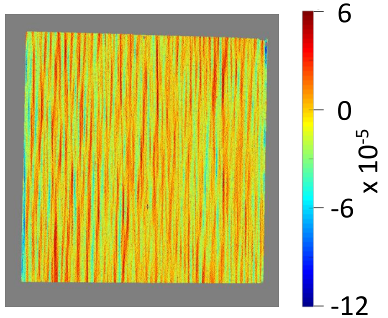

Y Curvature

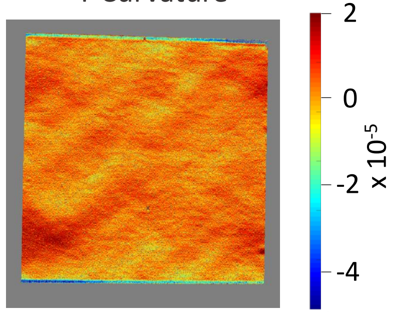

Error

Add: Design Reference

Ideal Design

$$z = \frac{x^2}{4f_x} + \frac{y^2}{4f_y}$$

$f_x = 100$ m

$f_y = 100$ m

$l_x = 1.22$ m

$l_y = 1.22$ m

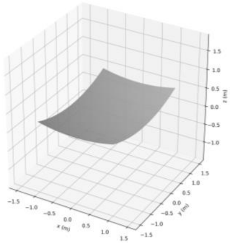

Slope Error Magnitude

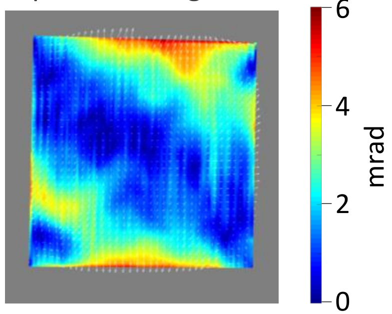

X Slope Error

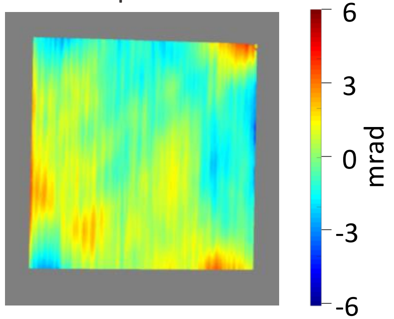

Y Slope Error

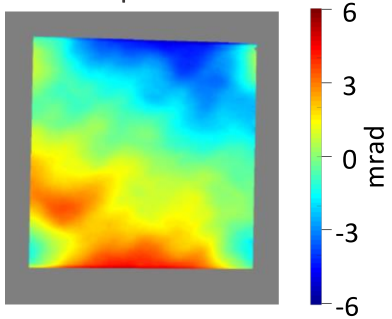

RMS slope error magnitude:	1.10 mrad
RMS slope error X:	0.51 mrad
RMS slope error Y:	0.97 mrad
Range slope error X:	[-TBD, + TBD] mrad
Range slope error Y:	[- TBD, + TBD] mrad
Best-fit focal length X:	TBD m
Best-fit focal length Y:	TBD m

Ray Trace

Add: Field Location, Target, Time

Field location:	[0.0 m, 95.7 m]
Target:	[0.0 m, 8.8 m, 28.9 m] BCS Wall

2022-06-30 14:40:22

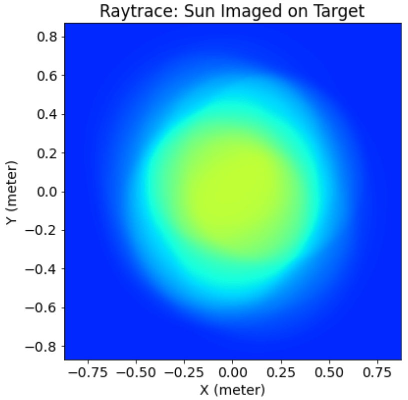

Output Summary: NSTTF Heliostat 5W01

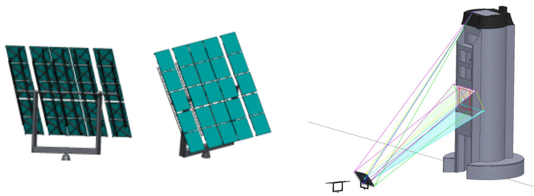

Absolute

Input: Measurement

Heliostat:	5W01
Instrument:	SOFAST Tower
Date/time:	2022-06-29 23:03
Sample points:	Grid
Number points:	4,446,000/heliostat 178,000/facet
Resolution X:	2.9 mm/pt
Resolution Y:	2.9 mm/pt
Uncertainty:	±TBD mrad

Slope Magnitude

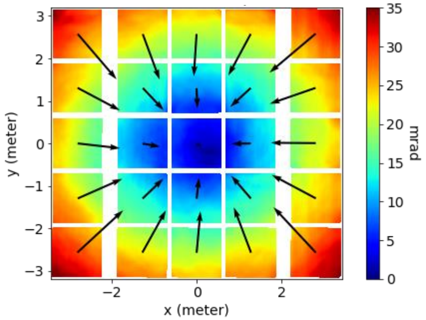

X Slope

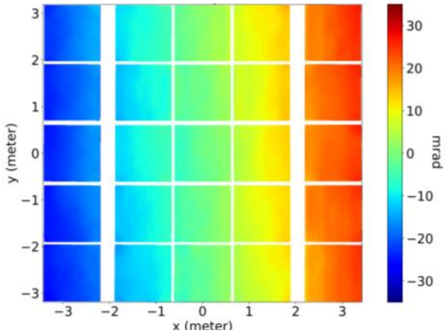

Y Slope

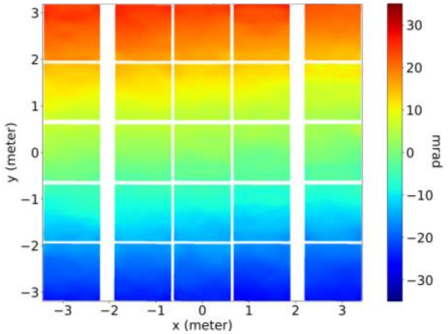

Curvature

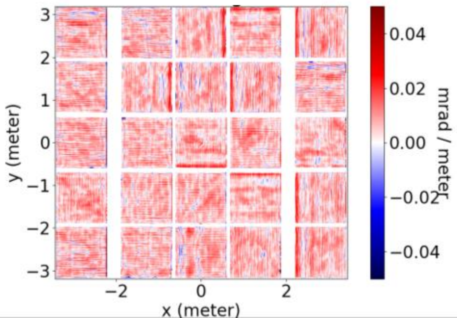

Error

Add: Design Reference

Ideal Design

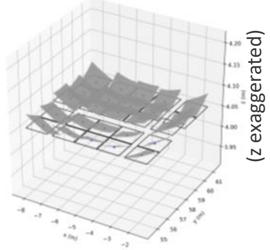

On-axis canting.
Slant distance 57.2 m.

Slope Error Magnitude

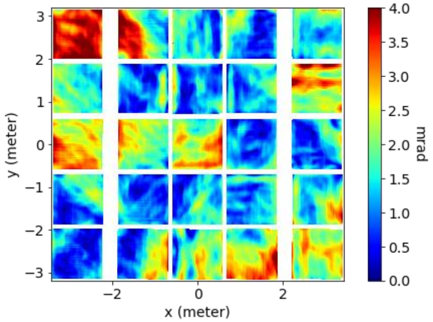

X Slope Error

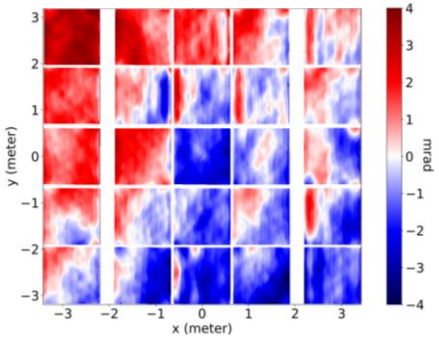

Y Slope Error

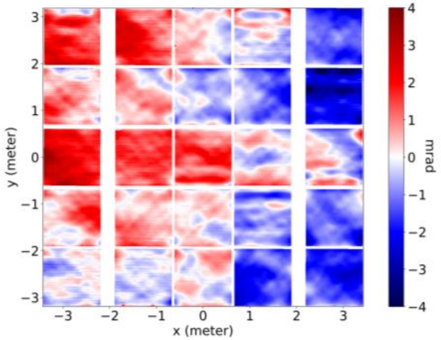

RMS slope error magnitude:	2.0 mrad	
RMS slope error X:	1.6 mrad	
RMS slope error Y:	1.3 mrad	
RMS canting error magnitude:	1.7 mrad	n = 25
RMS canting error X:	1.3 mrad	n = 25
RMS canting error Y:	1.2 mrad	n = 25
Range canting error X:	[-3.2, +2.0] mrad	
Range canting error Y:	[-2.5, +2.3] mrad	

Ray Trace

Add: Field Location, Target

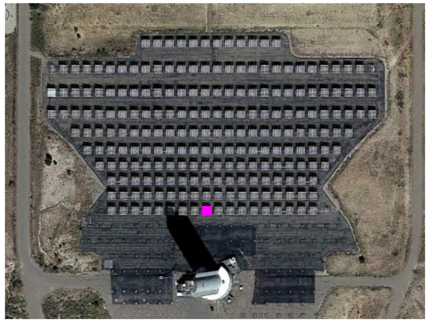

Field location: [-4.66 m, 57.9 m]

Target: [0.0 m, 8.8 m, 28.9 m]
BCS Wall

2022-06-30 14:06:09

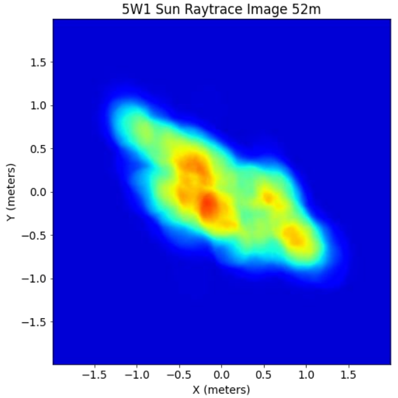

(After adjusting calibration)

Preliminary. Still work in progress.

Measurement Quality*

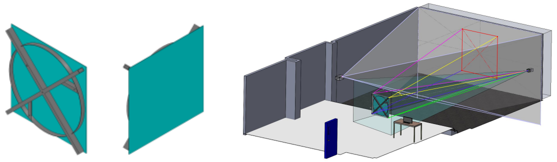

Resolution:

670 × 670
450,000 points
2 mm regular spacing
High-frequency detection

Precision:

pending
Depends on configuration

Accuracy:

Work in progress.

Cross-check with ground truth:

- 2f returned spot → agreement
- 2f color target → agreement
- Plano water pool → 0.17 mrad RMS
- Precision glass → pending

Automated uncertainty estimation → pending

Calibration refinement → pending

High-Frequency Detection

Example Reflection

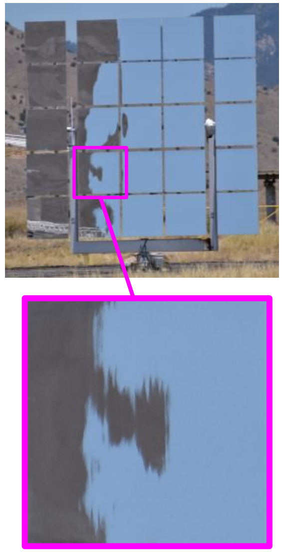

SOFAST Example (Different Mirror)

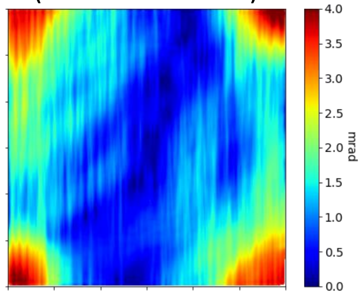

2f Returned Spot

2f Returned Spot Image

SOFAST Ray Trace

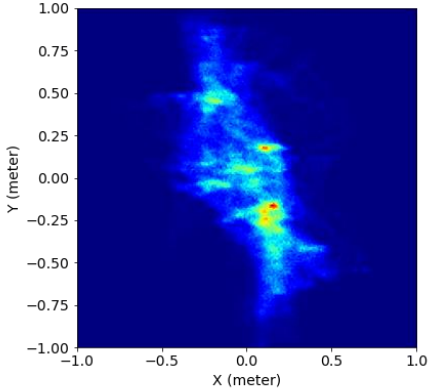

Images are same scale.

2f Color Target

2f Target Direct Image

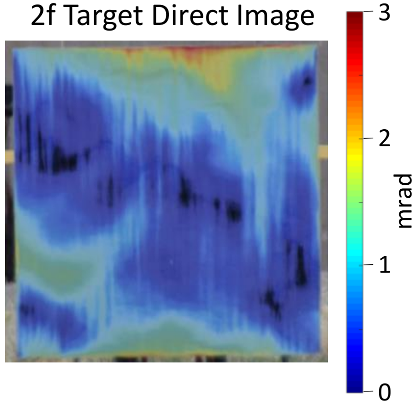

SOFAST Slope Error Magnitude

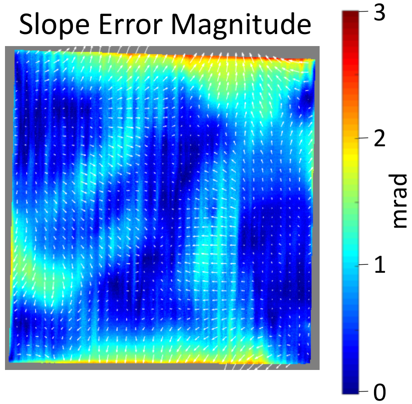

* All values are approximate, and specific to this example. Varies with mirror, configuration.
Green implies "still working on this."

On-Going Work

Addressing unsolved problems, creating new capabilities:

- Measure optical response under operating conditions. See backup slides.

Available for industry support

Education:

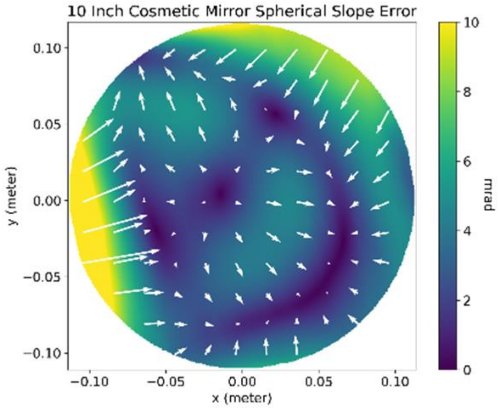

Increasing benefit:

- Ease of use.
- Industrial support.
- Educational version.
- Easy access – OpenCSP, Open SOFAST.

Our goal is to maximize benefit to CSP industry, research, education.

Conclusion

- SOFAST delivers rapid, high-resolution slope maps, supporting:
  - Prototype development.
  - High-volume manufacturing.
  - In situ inspection (limited).
  - Education.
- SOFAST is distortion-tolerant, and supports a variety of output analyses.
- Key limitations are the need for a large screen, a steady scene, ambient light control.
- We have been improving:
  - Flexibility – interactive CAD tool, reduced installation constraints, mobility.
  - Quality – code maintainability, automated testing, documentation.
  - Accuracy – developing ground-truth verification techniques.
  - Access – Python implementation, OpenCSP release planned.
- Ongoing work:
  - Automated sensitivity analysis.
  - Measure optical response under operating conditions.
  - Further develop SOFAST Tower, use as cross-check for other methods.

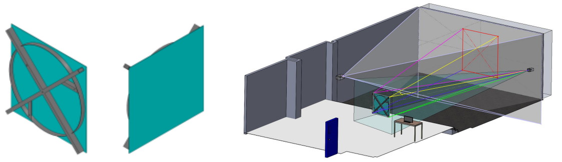

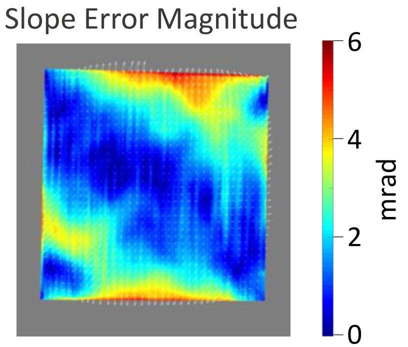

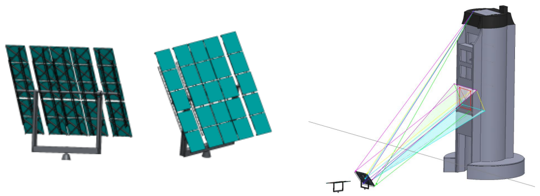

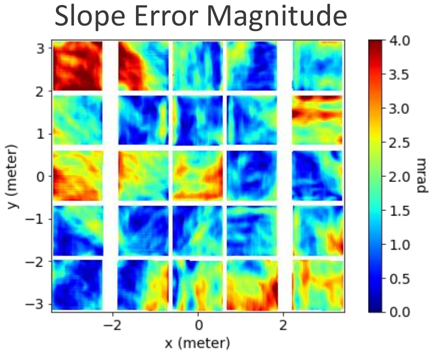

Our goal is to maximize benefit to the CSP community – industry, research, education.

BACKUP SLIDES

On-Going Work

Material for HelioCon Review

Addressing unsolved problems:

- Temperature optical effect?
- Tilt angle optical effect?
- Mobile SOFAST.

Available for industry support

Increasing benefit:

- Ease of use.
- Industrial support.
- Educational version.
- Easy access – OpenCSP, Open SOFAST.

Our goal is to maximize benefit to CSP industry, research, education.

Related work:

[1] Sartori, et al. Composite Mirror Shape Deviations Due to Temperature Changes. AIP Conference Proceedings **2303**, December 2023.

[2] Yuan, et al. Compensation of Gravity Induced Heliostat Deflections for Improved Optical Performance. *Solar Energy Engineering*, 2015.

Temperature:[1]

CFV Labs Chamber: -40°C → +85°C

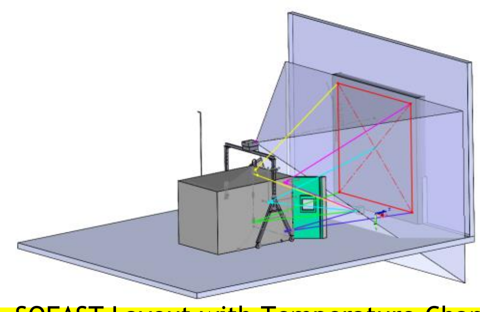

SOFAST Layout with Temperature Chamber

Tilt:[2]

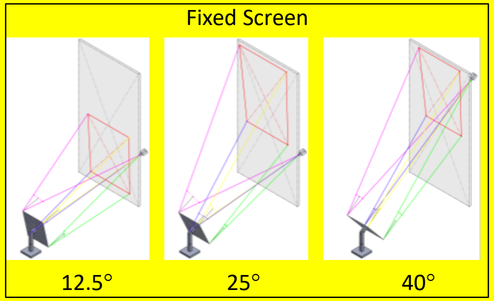

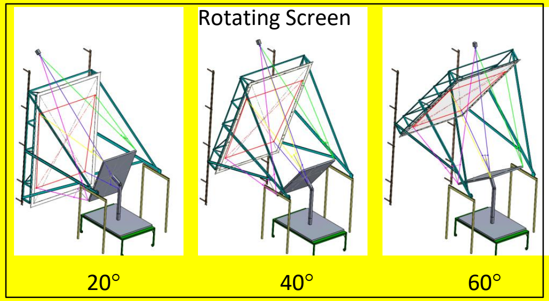

Mobile:

Education:

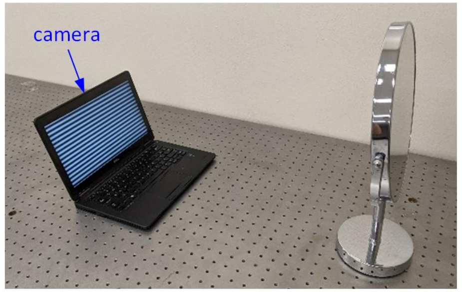

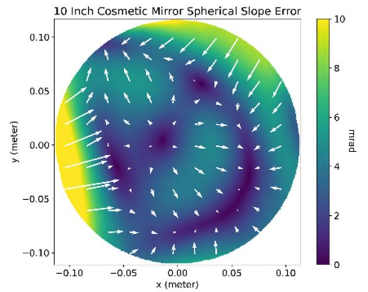

SOFAST Tilt – Fixed Screen

Limiting increments per camera position:

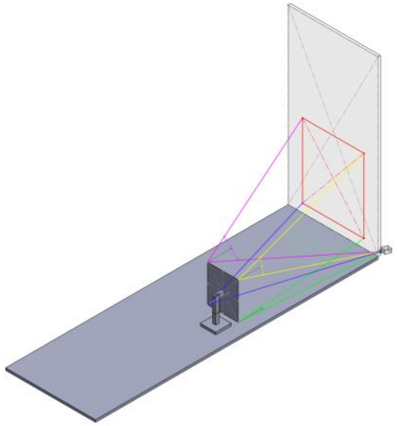

Camera 1
Elevation 0°

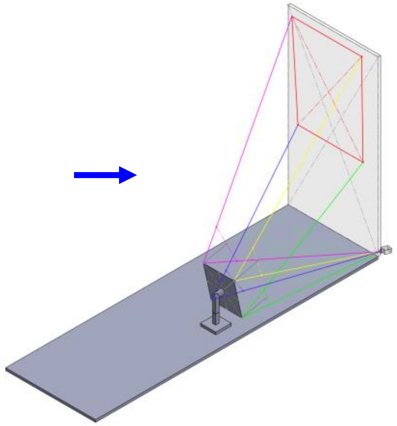

Camera 1
Elevation 12.5°

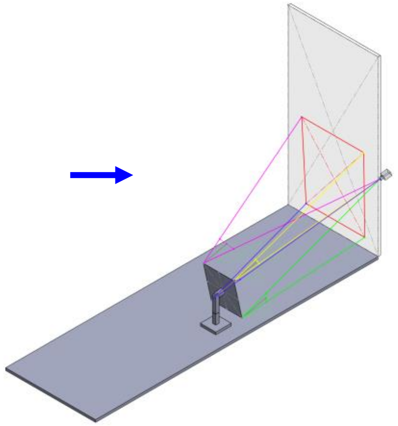

Camera 2
Elevation 12.5°

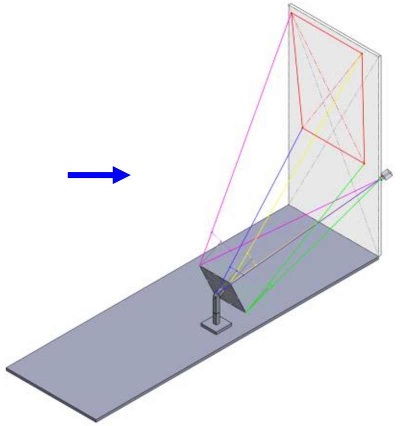

Camera 2
Elevation 25°

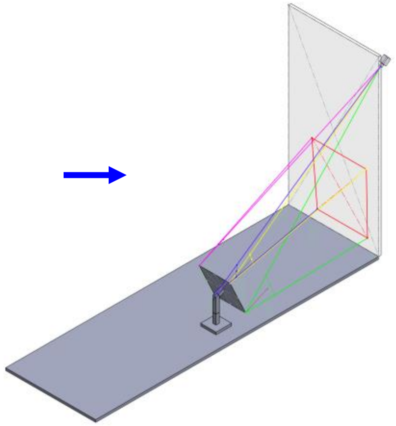

Camera 3
Elevation 25°

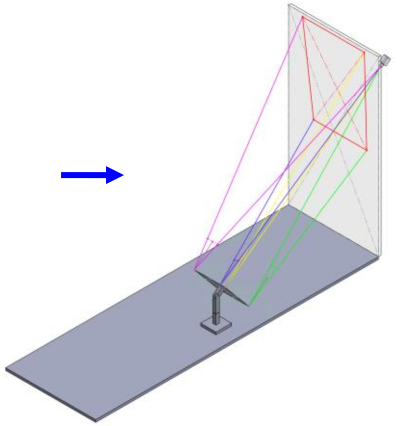

Camera 3
Elevation 40°

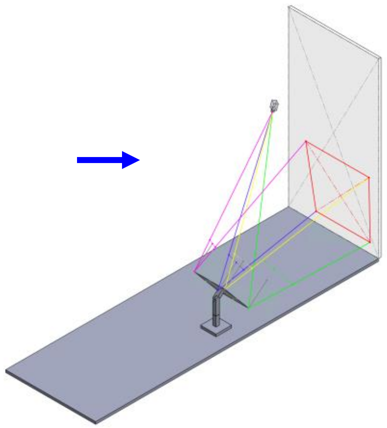

Camera 4
Elevation 40°

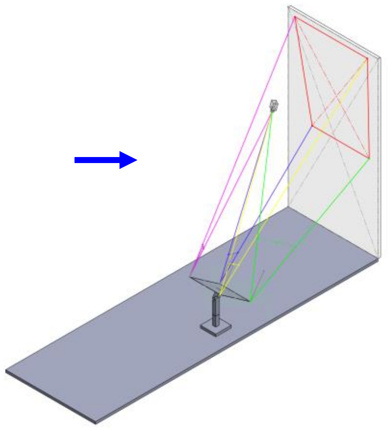

Camera 4
Elevation 55°

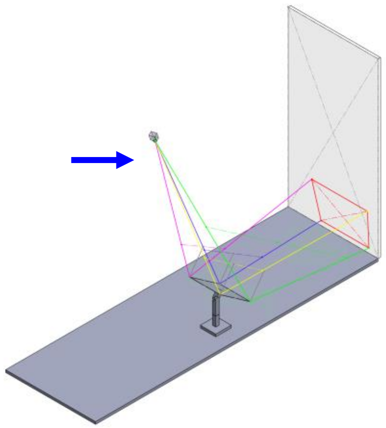

Camera 5
Elevation 55°

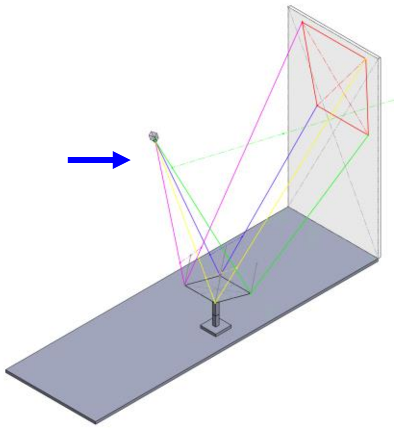

Camera 5
Elevation 75°

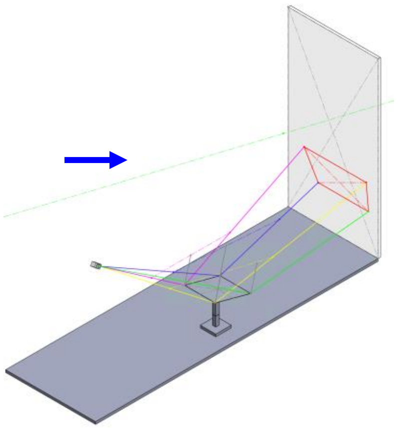

Camera 6
Elevation 75°

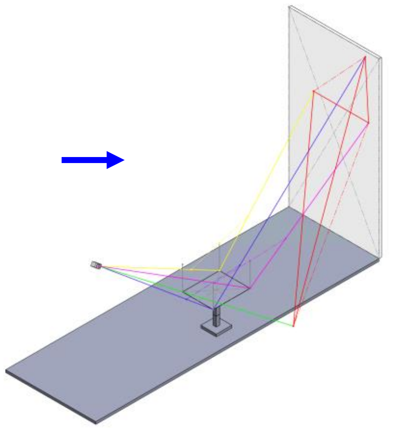

Camera 6
Elevation 90°

SOFAST Tilt – Rotating Screen

<ins>Example: 10° increments:</ins>

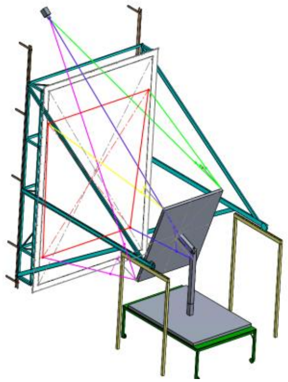
Elevation 20°
Screen 0°

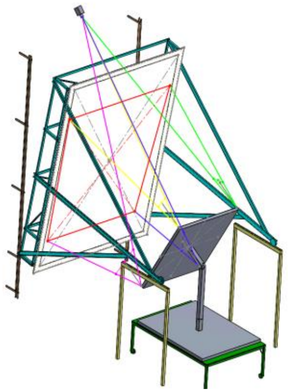
Elevation 30°
Screen 10°

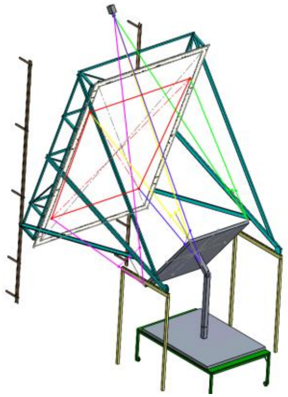
Elevation 40°
Screen 20°

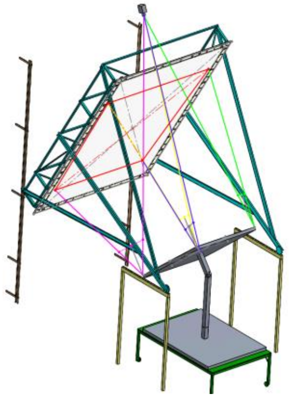
Elevation 50°
Screen 30°

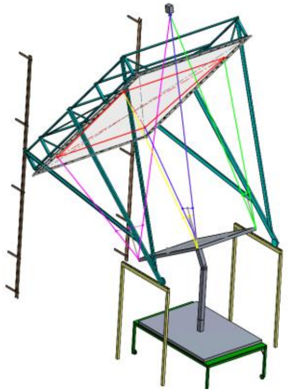
Elevation 60°
Screen 40°

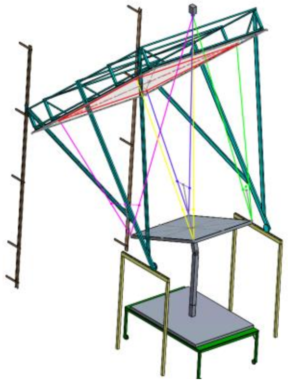
Elevation 70°
Screen 50°

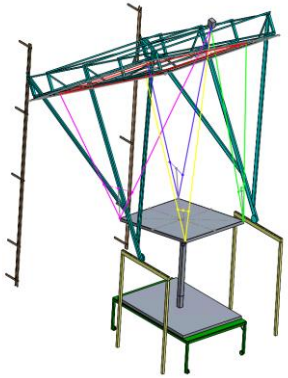
Elevation 80°
Screen 60°

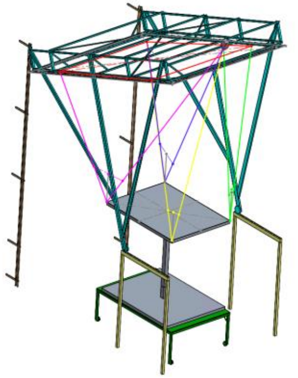
Elevation 90°
Screen 70°

Sensitivity: High Frequency

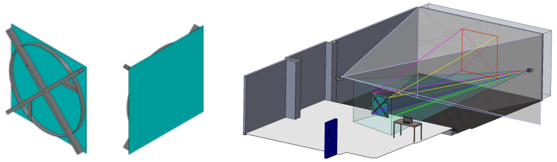

- We have observed high-frequency reflection effects in several mirrors from multiple manufacturers.
- These effects can influence reflectivity and energy production.
- SOFAST readily detects these effects, which other position-based metrology approaches may have a difficult time detecting.

NSTTF Tower

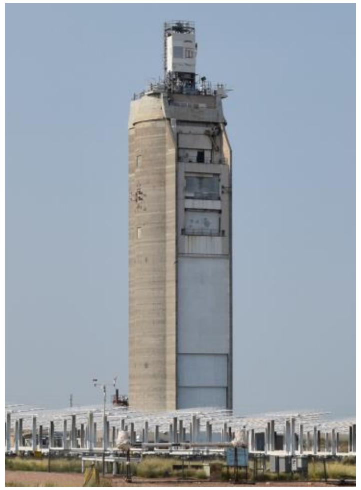

Tower Edge Seen in Reflection

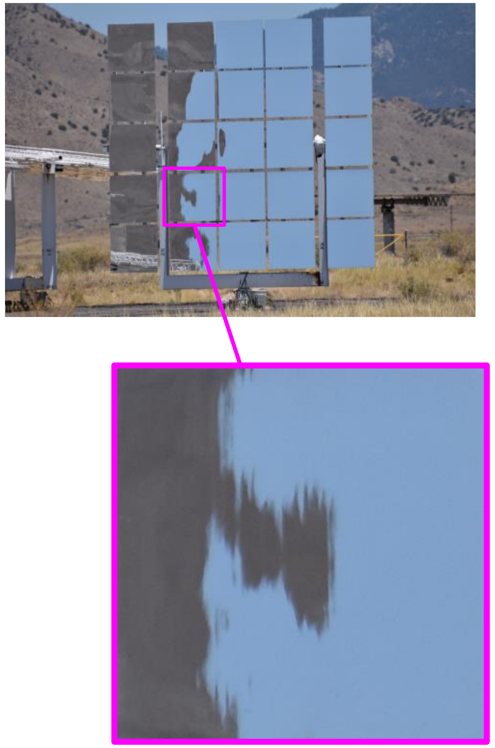

Example SOFAST measurement:

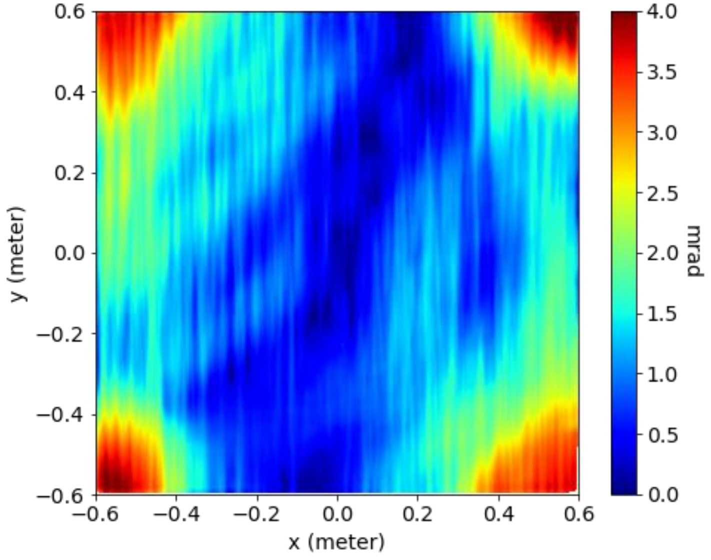

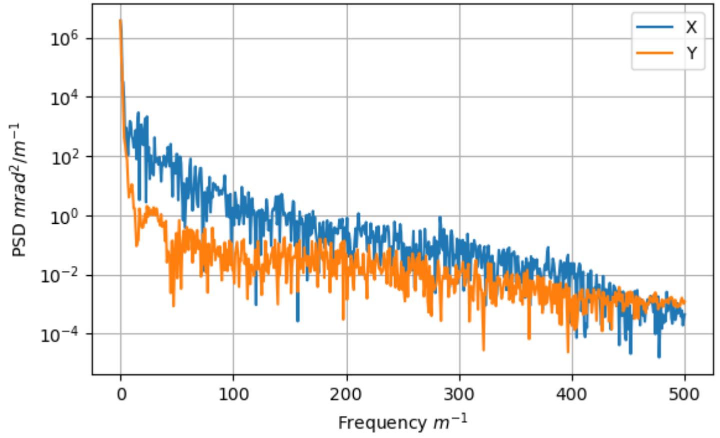

Sensitivity: Print-Through and High Frequency

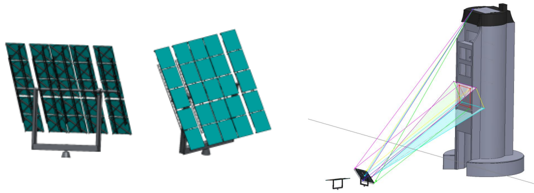

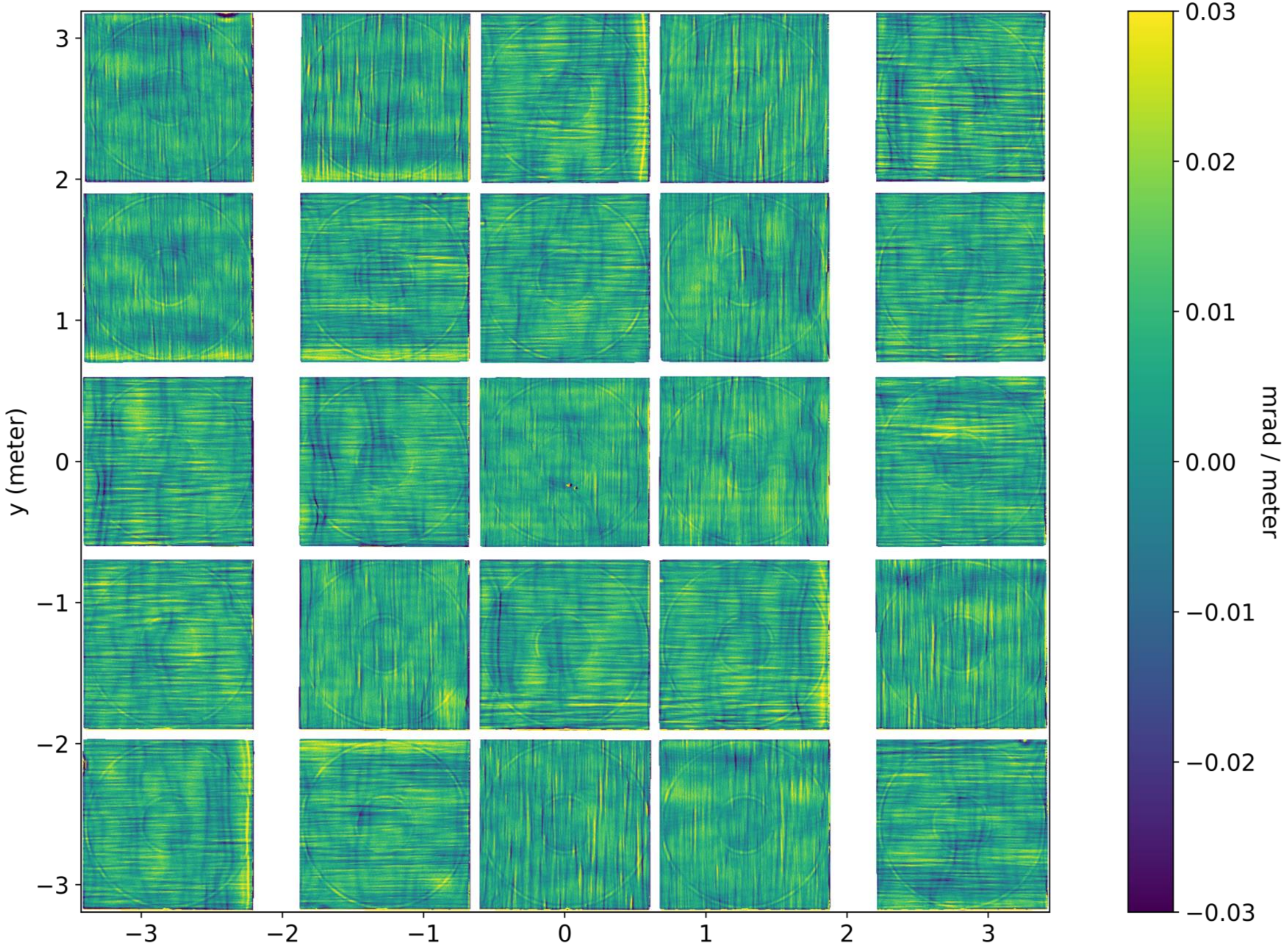

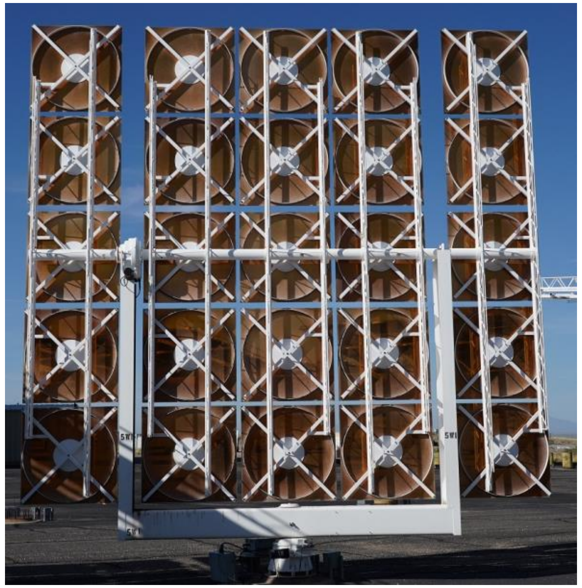

Heliostat Back Side

SOFAST is capable of detecting very fine features, both spatially across mirror, and in terms of slope deviation.

Ambient Light Variation

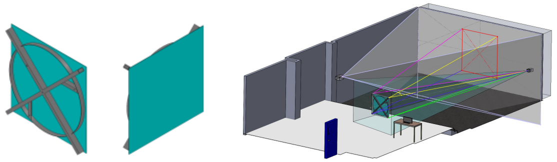

Background illumination reduces the available dynamic range for projecting fringes.

We measured the amount of background illumination in terms of “fringe visibility” v, instead of units such as lumens.

- $v = \left(\frac{I_{max} - I_{min}}{I_{max} + I_{min}}\right)$
- Visibility can take mirror/screen reflectivity into account when determining proper SOFAST illumination.

We found that SOFAST can produce accurate slope calculations for fringe visibilities > 0.6.

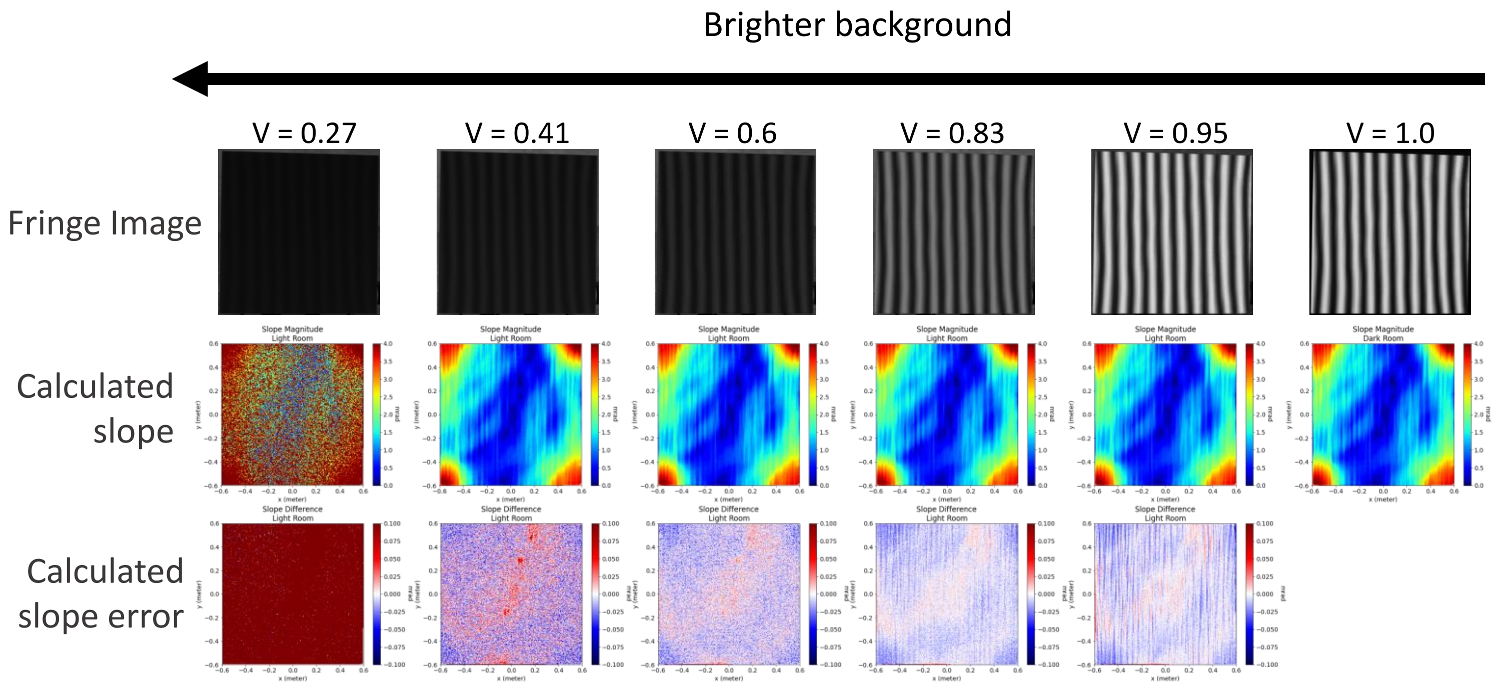

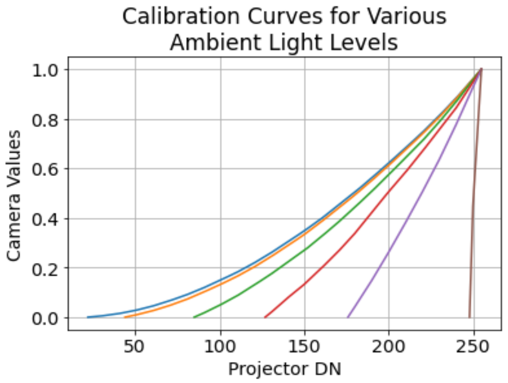

Calibration in dark room

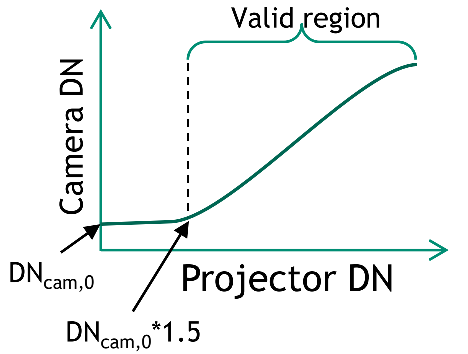

Calibration in light room

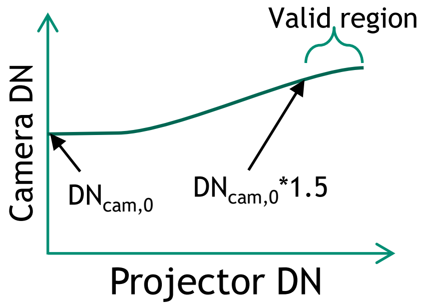

Ground Truth Methods

BCS

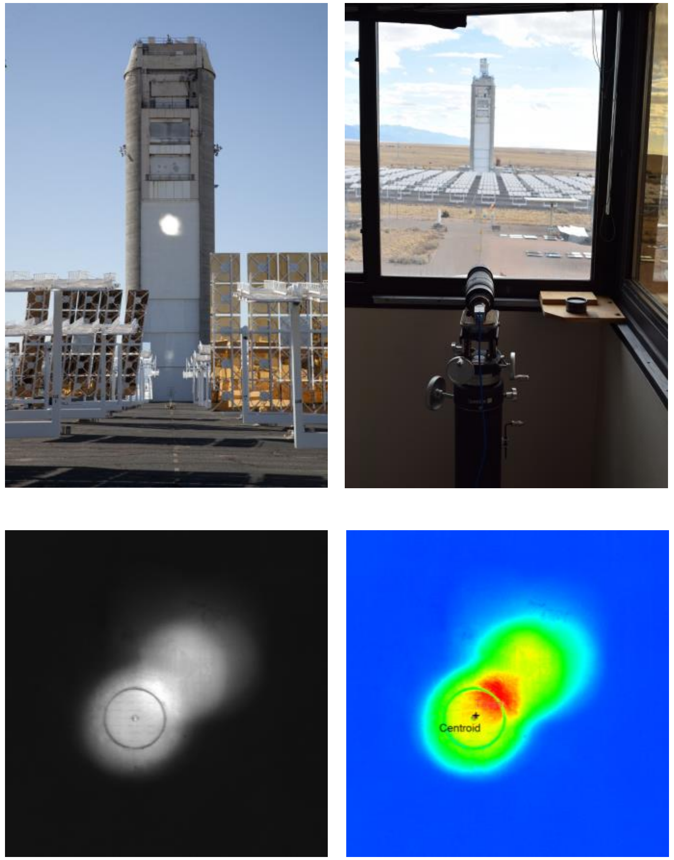

Direct measure of desired function.

Strachan's Observation[1]

For 100m focal length:

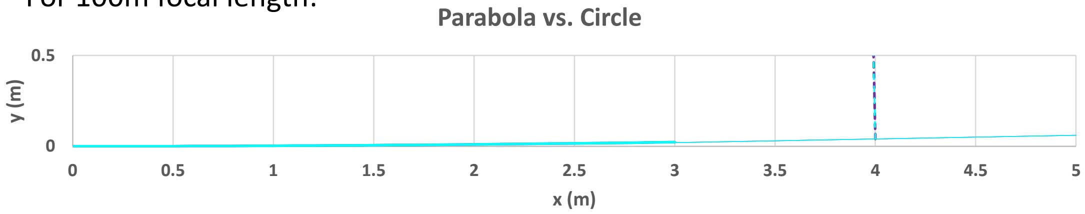

At 4 m aperture radius:

Focal Length (m)	Δ Slope (mrad)
100	0.00400
200	0.00050

2f Returned Spot

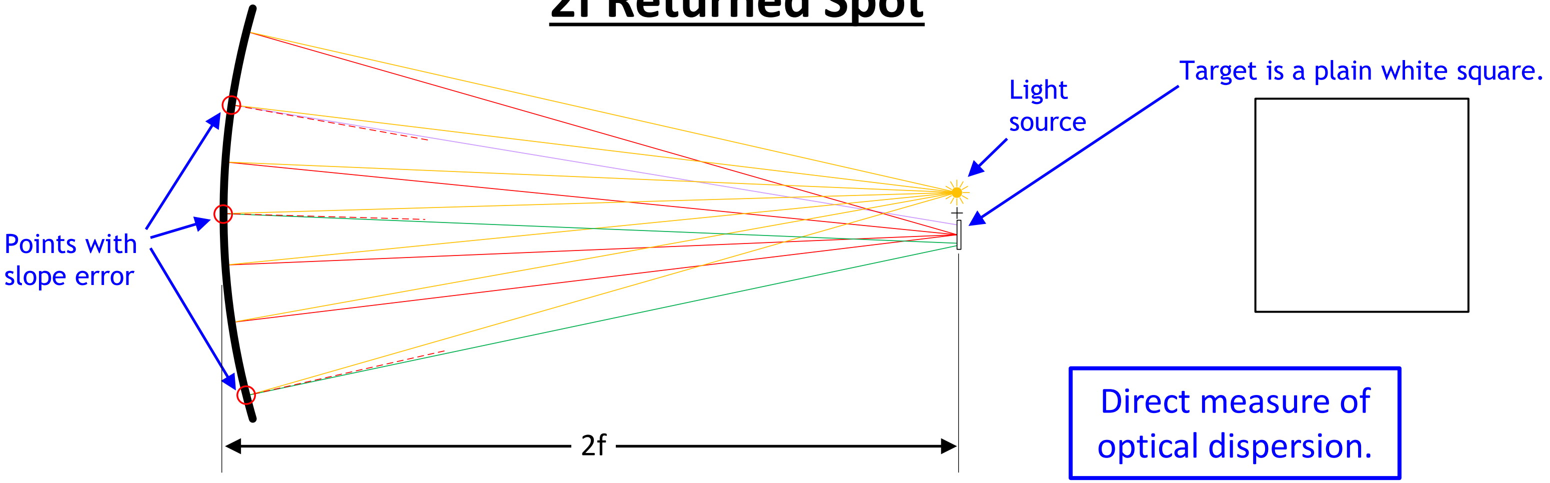

Direct measure of optical dispersion.

2f Color Target

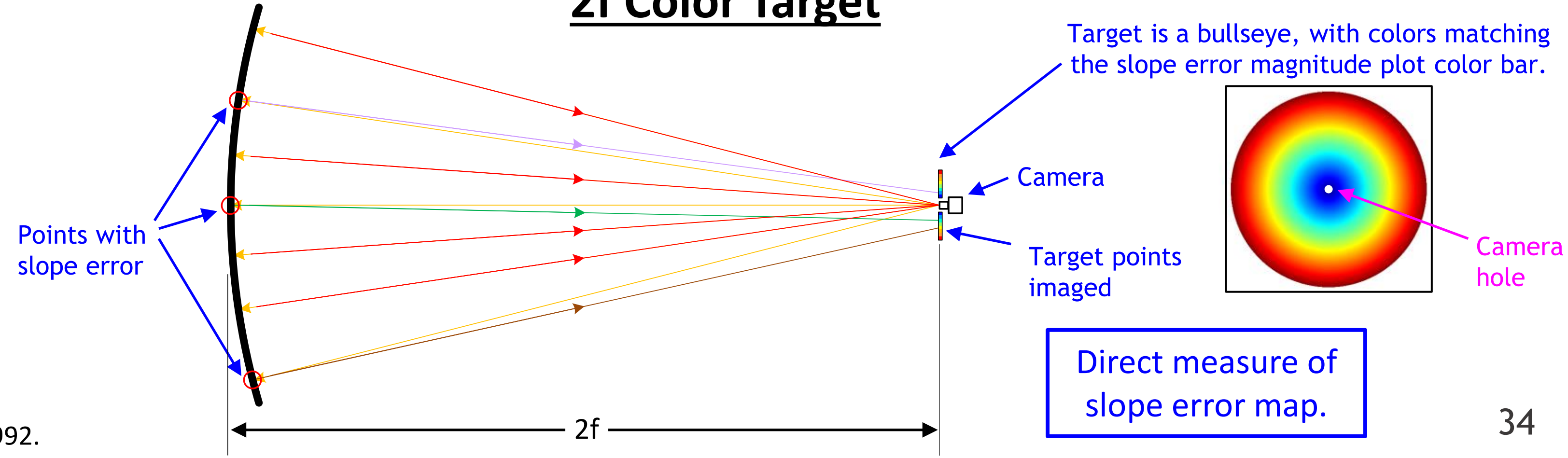

Direct measure of slope error map.

[1] J. Strachan. Revisiting the BCS…, Sandia Technical Report SAND92-2789C, 1992.

Ground Truth Check: NSTTF Facet

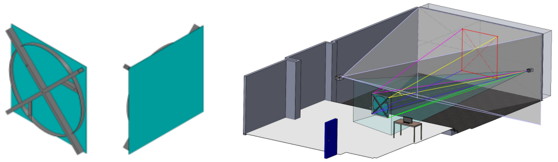

f = 100 m*

BCS

BCS Image

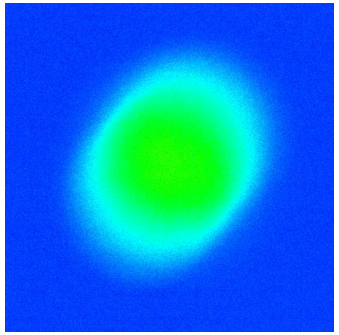

SOFAST Ray Trace

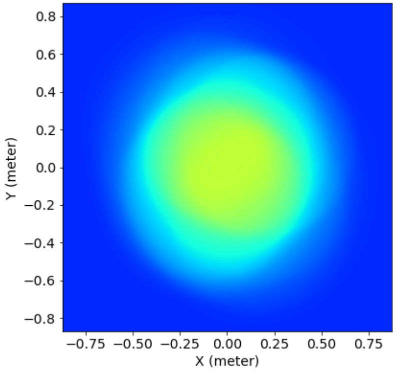

Images are same scale.

Image capture and ray trace both June 30, 2022 at 2:40 PM.

2f Returned Spot

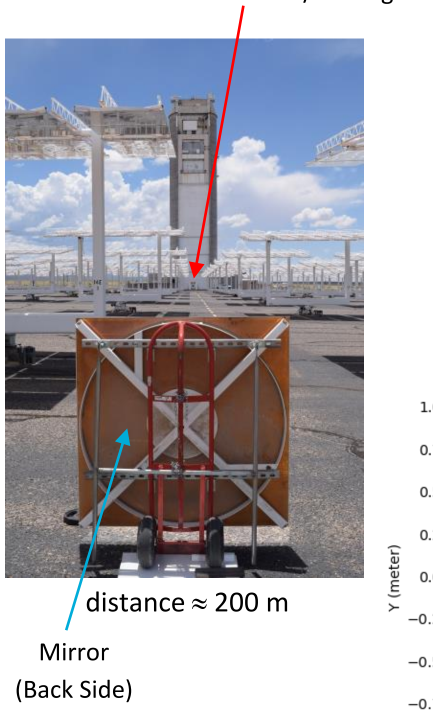

distance ≈ 200 m

2f Returned Spot Image

SOFAST Ray Trace

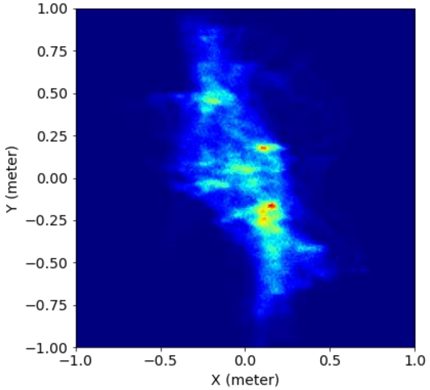

Images are same scale.

2f Color Target

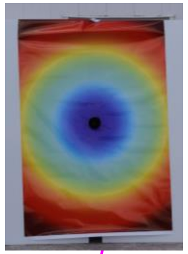

distance ≈ 200 m

2f Target Direct Image

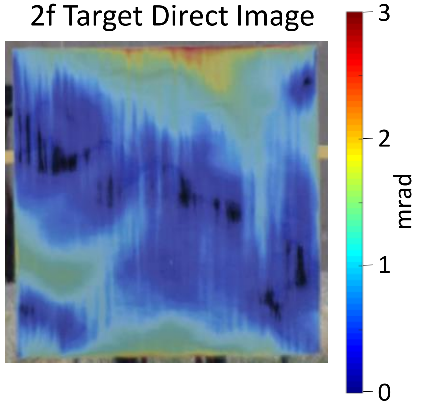

SOFAST
Slope Error Magnitude

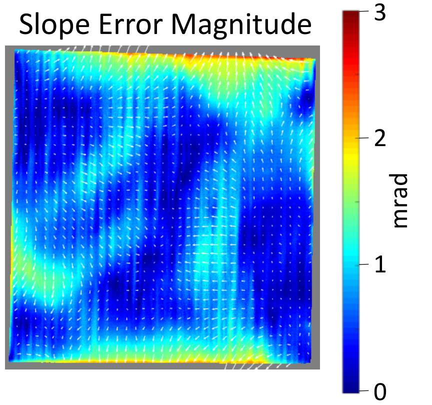

Quantitative comparison is work in progress.

* NSTTF facets are adjustable. SOFAST was used to set focal length to 100 m, as measured by SOFAST.

Ground Truth Physical Standards

- Ground truth physical standards are objects where you know what the measurement result should be. If you use an instrument to take a measurement and the answer is not what's expected, you know the problem is with the instrument.
- The best physical ground truth standards are low cost and easy to replicate anywhere – a Dewar with ice water for calibrating temperature is a familiar example.
- Other ground truth physical standards are standard references that are prepared by laboratories with certified equipment. These need to be checked periodically to ensure that they have not degraded.
- We are pursuing ground truth standards of both kinds.

  1. A **plano water pool** is easy to replicate and reliable if vibrations are not present. This appears well-known in CSP (e.g., T. März, et al. 2011). It has two disadvantages:
     - It only works face-up, and cannot be used to calibrate instruments that measure mirrors in other orientations.
     - It has virtually zero curvature, and thus cannot be used to assess an instrument's ability to measure curvature – an important aspect for CSP metrology.
  2. We are purchasing a **high-quality concave mirror** produced by a manufacturer of optics made to imaging tolerances. It is a monolithic glass disk 625 mm in diameter and 40 mm thick, with a concave spherical optical surface with a curvature radius R = 200 m, corresponding to a 100 m focal length. We have placed a contract with Cosmo Optics, and delivery is expected sometime this summer.

     The returned spot test will be a simple, effective method for checking the mirror.

Plano Water Pool

f = 100 m Calibration Mirror Design

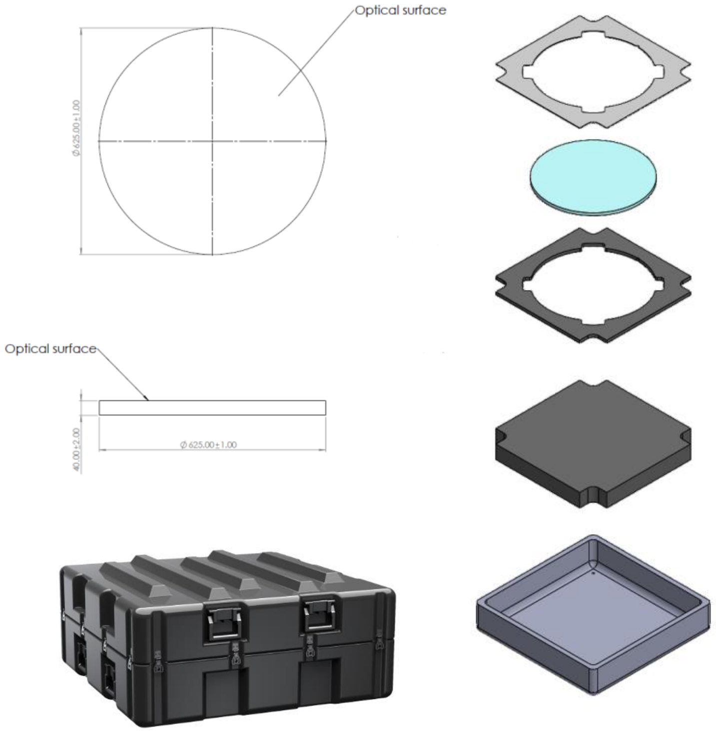

Plano Water Pool Test

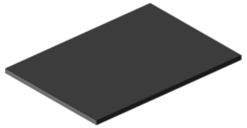

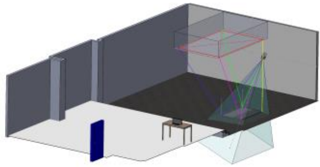

Water pool ground truth measurement done on March 8, 2023.

Improvements:

- Better water setup.
- A photogrammetric screen calibration was done the same day.
- No occlusions in field of view of water pool.

Notes:

- Calibration parameters were optimized via gradient descent algorithm.
- Fitting equation was constrained to plano surface.

X RMS: 0.131496 mrad
Y RMS: 0.113820 mrad
Magnitude RMS: 0.173914 mrad

Optimized Slope Map

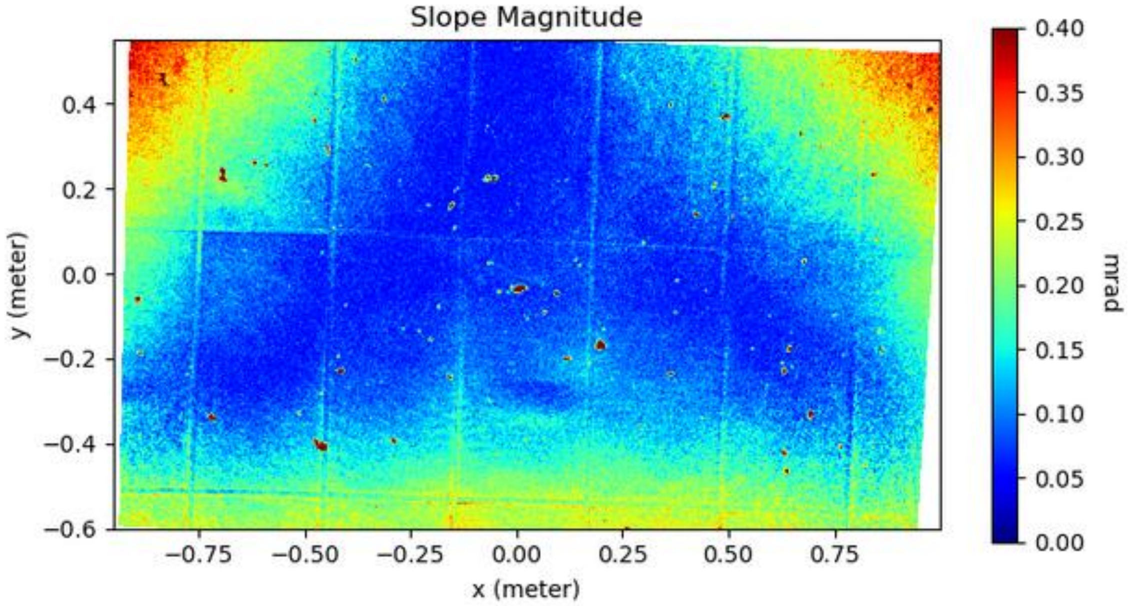

Corner errors of 0.4 mrad are high. Work in progress.

Distortion Tolerance

- CSP mirrors can exhibit highly distorted reflections.
- Feature-based correspondence methods are vulnerable to confusion in mapping, given a distorted image.
- In contrast, SOFAST uses a pixel-based correspondence mapping scheme which is fundamentally immune to distortion.

<u>Distortion Example</u>

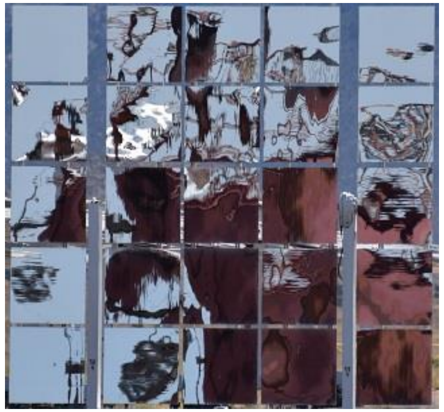

Reflected distortion depends on conditions.

<u>Feature-Based Correspondence</u>

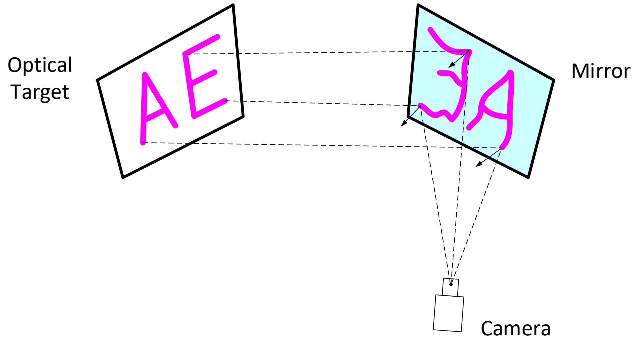

Excessive distortion can cause feature recognition to fail.

<u>SOFAST Fringes and Distorted Reflection</u>

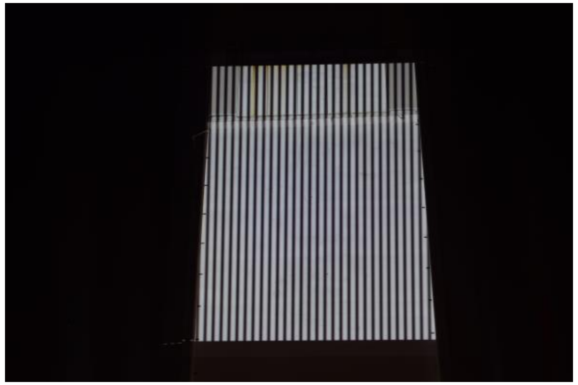

Not a problem for SOFAST.

CSP Mirror Distortion Effects

Varying Heliostat-to-mirror and camera-to-mirror distance:

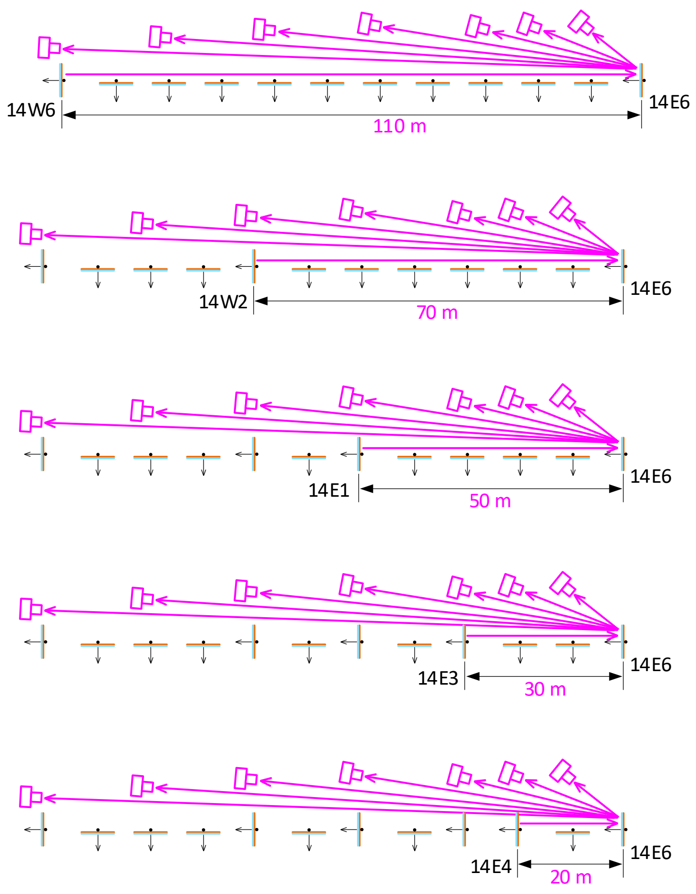

Photograph, then crop

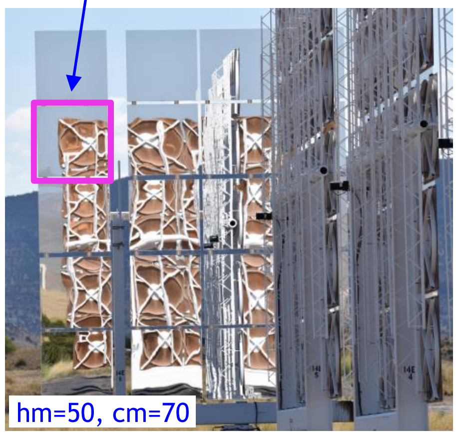

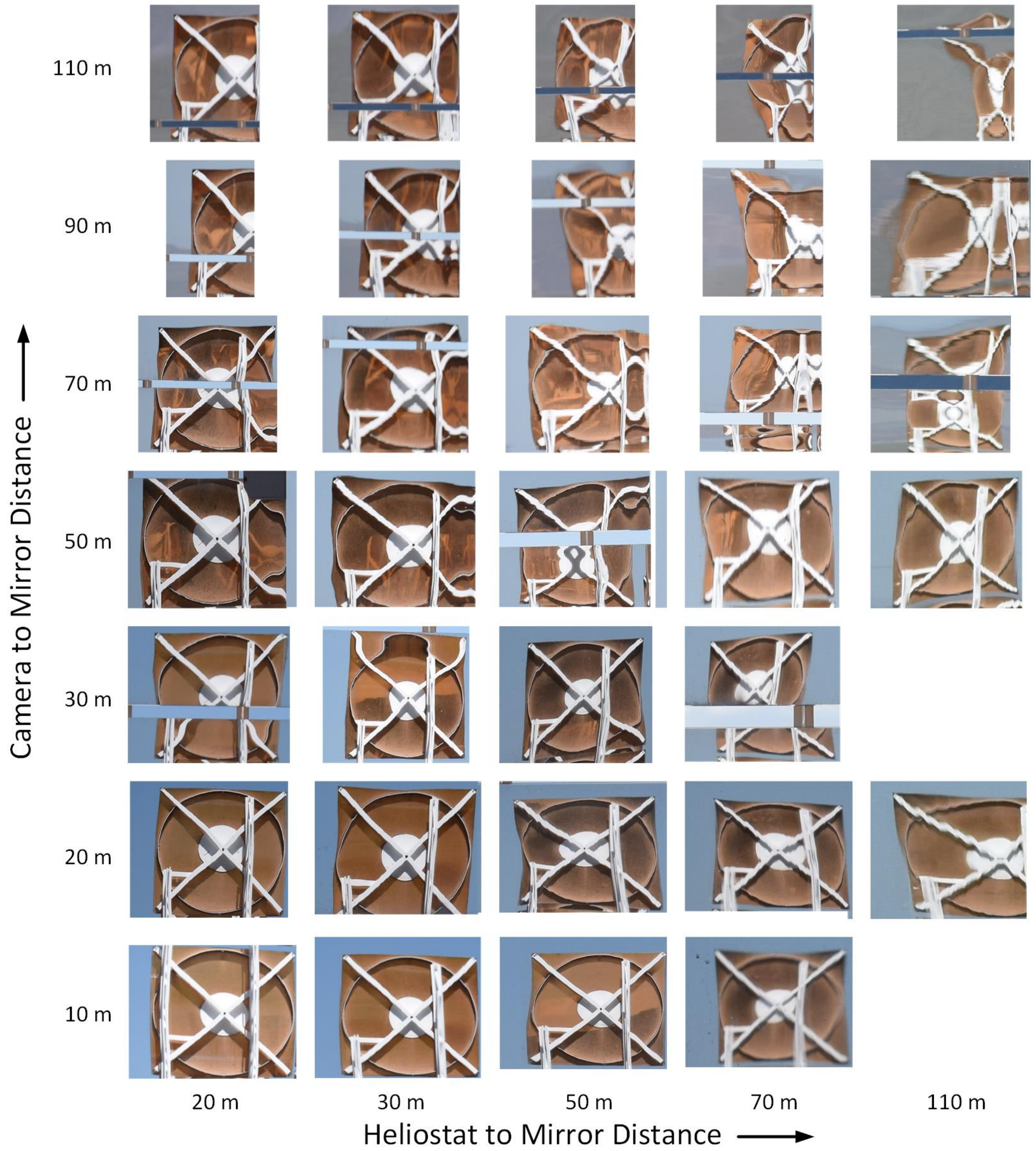

Conclusion:
Distortion increases with heliostat-to-mirror distance, and also with camera-to-mirror distance.

Tower-to-Mirror Distortion

Single facet method:

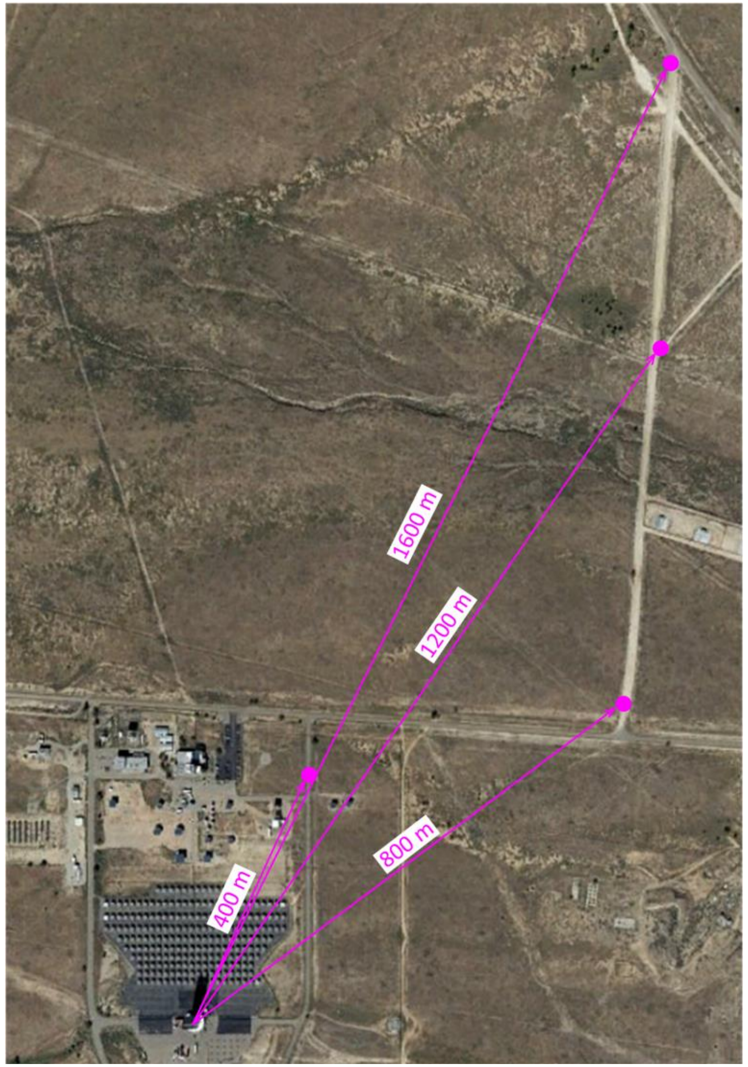

Images captured at 25, 50, 100, and 150 m from the mirror.
Lateral moves at each point, to simulate UAS scan.

Flat mirror

Photograph, then crop to facet

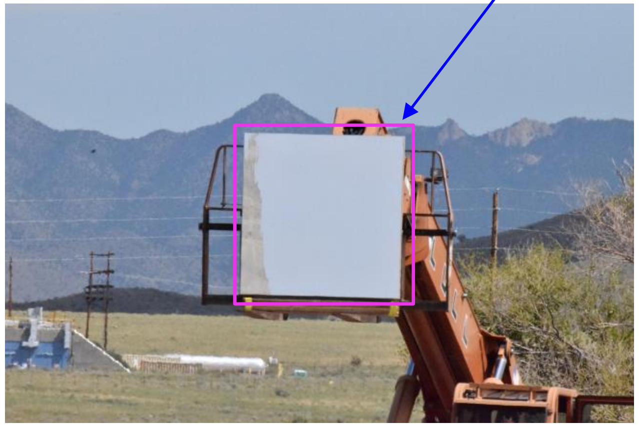

A flat mirror was used, so that:
(a) Non-imaging optic distortion would not occur, and
(b) Focal length mismatch would not be an issue.

Distortion: Tower-to-Mirror vs. Camera-to-Mirror Distance

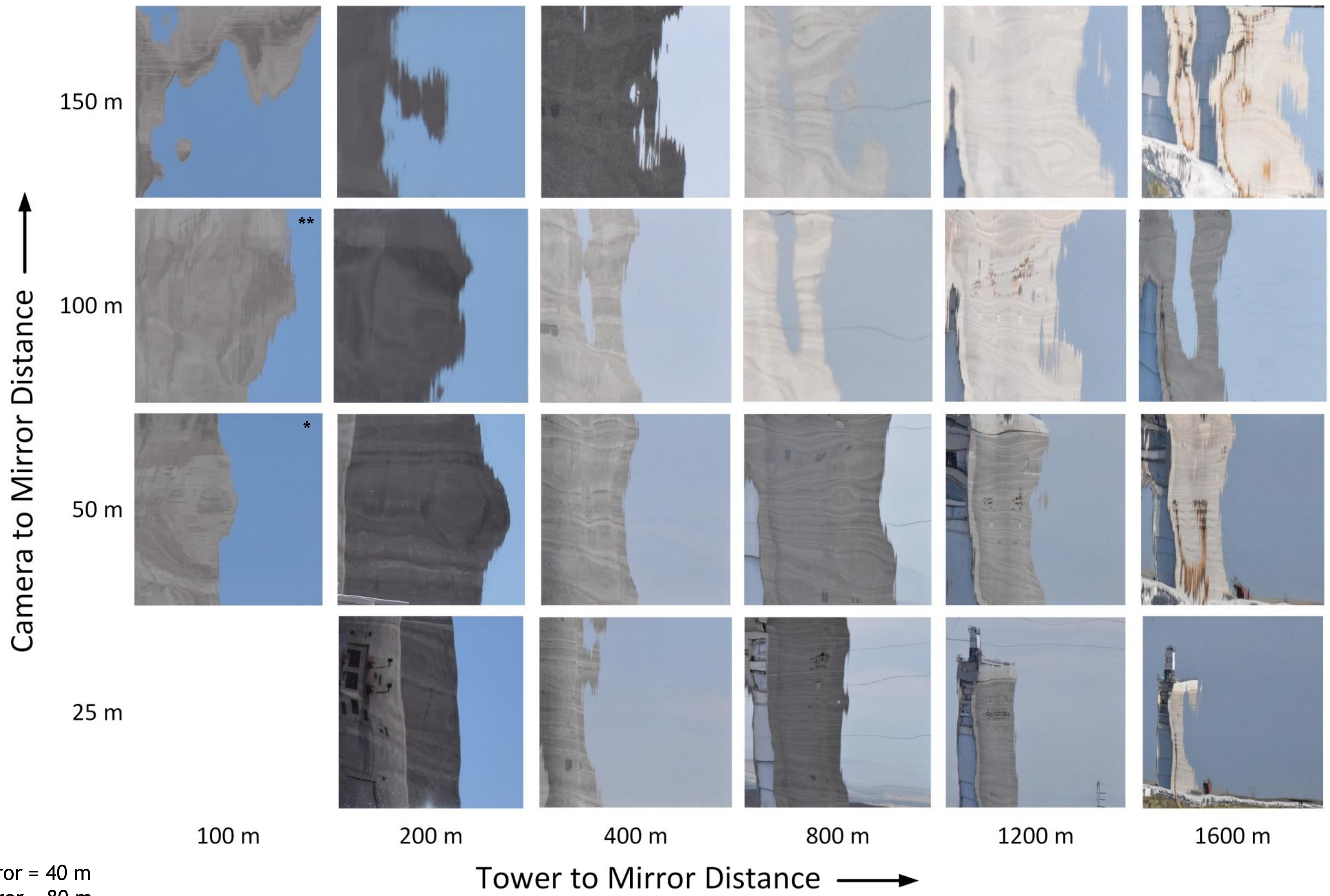

Conclusion:
We see distortion increase with camera-to-mirror distance, but we do not see a clear increase with tower-to-mirror distance.

Why?

* camera-to-mirror = 40 m
** camera-to-mirror = 80 m

Modeling Mirror Distortion

One step in a series:

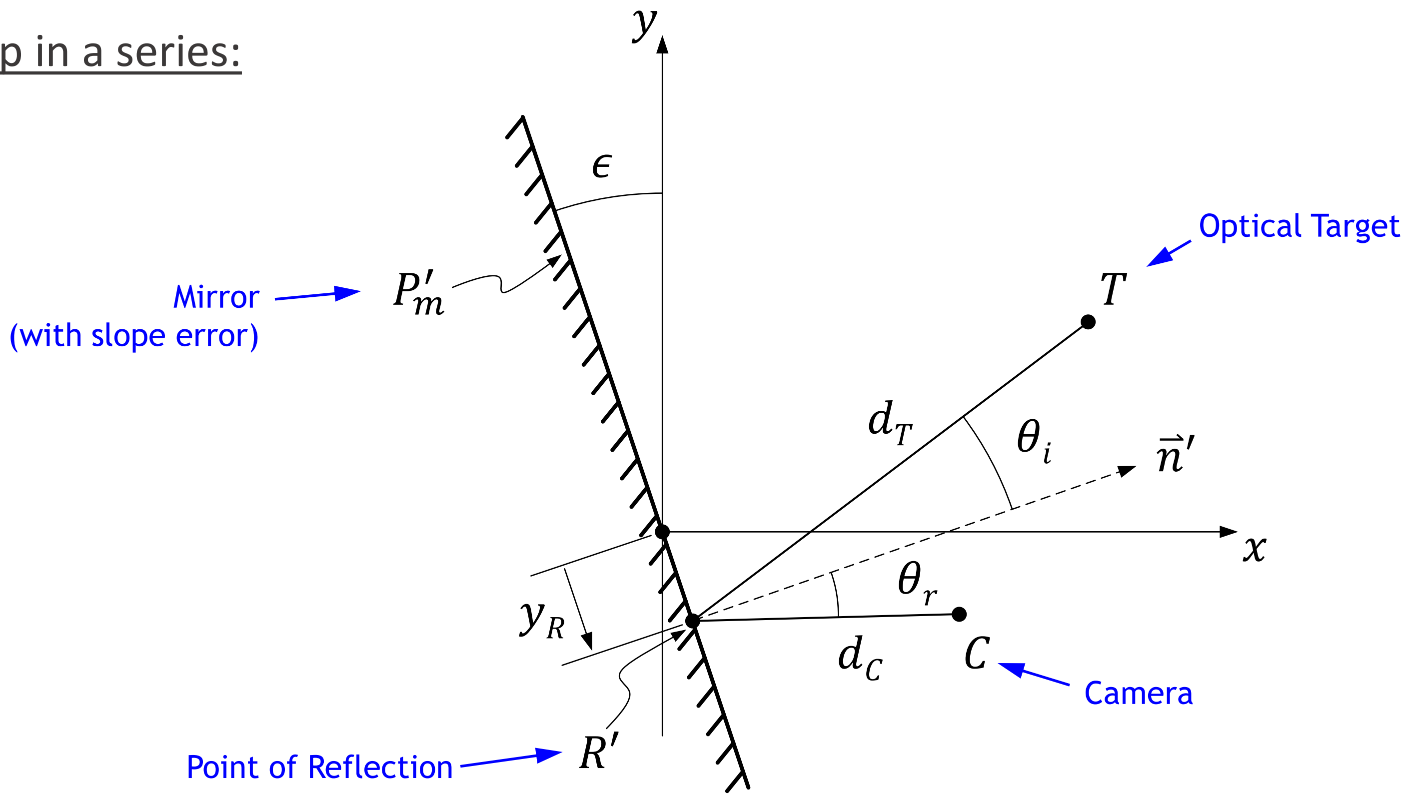

After several derivation steps:

$$y_R = \frac{-2\, d_T d_C \cos(\epsilon)\sin(\epsilon)}{d_T \cos(\theta_i - \epsilon) + d_C \cos(\theta_i + \epsilon)}$$

Computer verification:

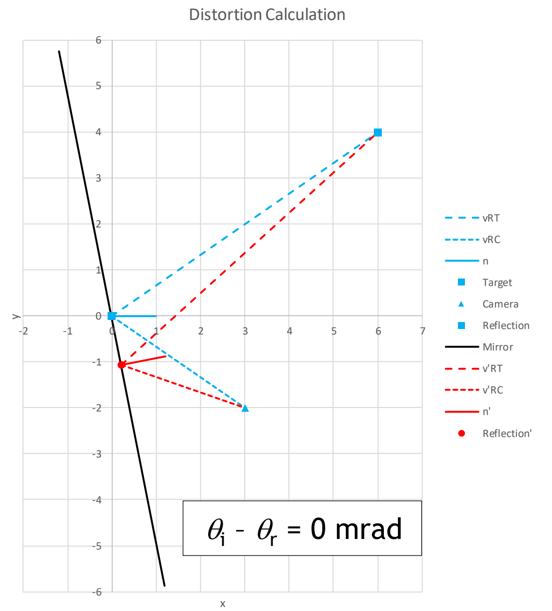

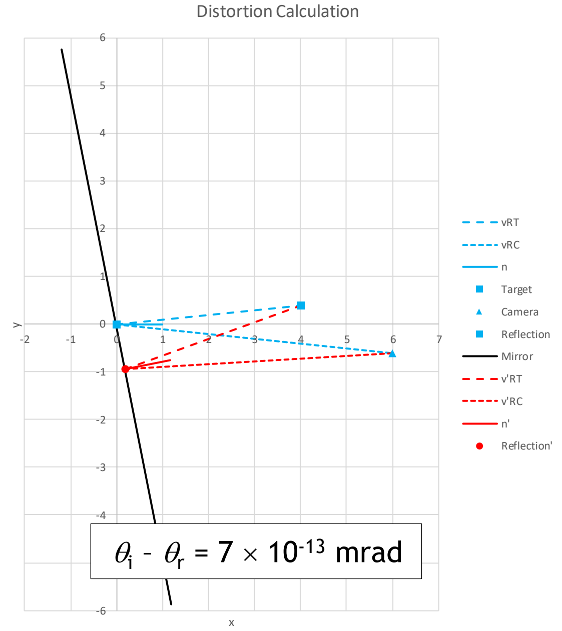

Modeling Mirror Distortion

<u>If slope errors are small:</u>

Main result

$$y_R = \frac{-2\, d_T\, d_C\, \epsilon}{cos(\theta_i)[d_T + d_C]}$$

1. Sign of the error is correct for our example.
2. Distortion grows linearly with slope error ϵ. (Within small angle assumption)
3. As the incidence angle θ_i becomes very high, distortion grows rapidly.
4. Distortion grows with both target-to-mirror and camera-to-mirror distance.
5. Distortion grows rapidly (with the square) of the total optical path length.
6. Both target-to-mirror and camera-to-mirror distance have a symmetric effect on distortion, if both are similar magnitude.

<u>If $d_T >> d_C$:</u>

$$y_R = \frac{-2\, d_T d_C\, \epsilon}{cos(\theta_i)[d_T + d_C]} \quad [d_T + d_C] \approx d_T \quad \Rightarrow \quad y_R = \frac{-2\, d_C \epsilon}{cos(\theta_i)}$$

7. Matches long-distance tower-to-mirror observations.

<u>This explains our observations:</u>

1. For heliostat-to-heliostat reflections, distortion grows with both target-to-mirror and camera-to-mirror distance.
2. For tower-to-mirror reflections, distortion grows primarily with camera-to-mirror distance.

<u>Computer verification:</u> Approximation error for ϵ = 10 mrad: 0.004%, 0.0002% for two cases studied. (Percentages calculated with respect to smaller of d_T, d_C.)

Legal Notice

Sandia National Laboratories is a multi-mission laboratory managed and operated by National Technology & Engineering Solutions of Sandia, LLC (NTESS), a wholly owned subsidiary of Honeywell International Inc., for the U.S. Department of Energy's National Nuclear Security Administration (DOE/NNSA) under contract DE-NA0003525. This written work is authored by an employee of NTESS. The employee, not NTESS, owns the right, title and interest in and to the written work and is responsible for its contents. Any subjective views or opinions that might be expressed in the written work do not necessarily represent the views of the U.S. Government. The publisher acknowledges that the U.S. Government retains a non-exclusive, paid-up, irrevocable, world-wide license to publish or reproduce the published form of this written work or allow others to do so, for U.S. Government purposes. The DOE will provide public access to results of federally sponsored research in accordance with the DOE Public Access Plan.